HHS Public Access

Author manuscript

IEEE Trans Robot. Author manuscript; available in PMC 2020 February 01.

Published in final edited form as:

IEEE Trans Robot. 2019 February ; 35(1): 35–48. doi:10.1109/TRO.2018.2875421.

Navigation Functions with Time-varying Destination Manifolds in Star-worlds

Caili Li [Student Member, IEEE] and **Herbert G. Tanner [Senior Member, IEEE]**

Department of Mechanical Engineering, University of Delaware, Newark, DE, 19711 USA

Abstract

This paper formally constructs navigation functions with time-varying destinations on star worlds. The construction is based on appropriate diffeomorphic transformations and extends an earlier sphere-world formulation. A new obstacle modeling method is also introduced, reducing analytical complexity, and offering unified expressions of common classes of n-dimensional obstacles. The method allows for dynamic target tracking, and is validated through simulations and experiments.

Keywords

Navigation functions; target tracking; dynamic environments; moving goal

I. Introduction

By now, the problem of *feedback-based* motion planning in fixed and known enviromnents [1] is well understood and adequately treated. When the workspace topology is known, and both environment and robot destinations are fixed (i.e. time-invariant), we know how to construct feedback controllers based, say, on navigation functions [2], to provably obtain (almost) global convergence to those destinations. Destination configurations, however, may not always be fixed within obstacle enviromnents. Examples can be found in applications ranging from detecting radiation sources in transit, to pediatric rehabilitation. In both of the aforementioned cases, a pursuing robot should maintain some small but safe distance from its target. Even when the trajectory of the goal configuration is known, the *combination* of stationary obstacles and moving destination does not necessarily fit the standard time-invariant analysis which establishes that the potential field is local minima-free.

Many variants of the potential field approach have been introduced to address the motion planning problems for both mobile robots [3]–[5] and manipulators [6], [7]. However, all classical (attractive & repulsive) potential fields [8] suffer from local minima problems [9]. Although several improvements have been proposed, (fuzzy logic [10], [11], simulated annealing [12], intermediate goals, or by combinations of sampling-based or search-based path planners [13]–[16]), no method can provide probably complete solutions without significant performance degradation.

Admittedly, a reference vector field does not necessarily have to be derived from a potential function. Instead, it can be explicitly defined over the state space; although in such a case, additional techniques are usually required to achieve global convergence *with* obstacle avoidance. In fact, methods of this type—like passive velocity field control, used for robot manipulators manipulators in contour following [17]–[19], and mobile robots in tracking moving targets [20], [21]—have been used for dynamic motion planning, but in obstacle-free environments. One avenue to incorporate obstacles is workspace discretization [22]; although effective in general, such approaches are subject to the curse of dimensionality, in addition to linking accuracy to discretization resolution.

If one allows for workspace discretization, a realm of alternative to potential field-based solutions are available; for example, *search-based algorithms* [23]. Search-based methods usually require the motion planner to renew the search every time the configuration space changes. Within this realm, *sampling-based methods* play an important role, offering computational savings by avoiding the explicit construction of obstacles in the state space [24]; however, only probabilistic completeness guarantees can be expected. For most alternative (i.e. not based on exhaustive search or sampling) navigation approaches, approximations [25] and elaborate collision detection algorithms may be needed. Since now one is outside the domain of potential fields, the navigation problem would typically be decomposed into (a) reference path or trajectory generation, and (b) local tracking. This decomposition requires a separate solution, or planner, for each subproblem [26]. And while feedback may still be incorporated locally in those planners, usually little can be said (deterministically) about global convergence and completeness.

Turning for this reason our attention back to potential-field-based methods, we can distinguish two approaches that address the local minima problem directly: *Harmonic functions* [27] and *navigation functions* [2] (Fig. 1). Harmonic functions are solutions of Laplace equation, available for convex hull approximations of 2D planar obstacles [28], [29]. Feedback controllers based on harmonic functions have been designed for dynamic environments [30], [31] For harmonic fields, there is no simple and general analytical obstacle modeling method; even planar cases involve intensive integral computations. Alternative to harmonic functions, yet still within the class level-set based methods, are *fast marching* methods [32], which produce scalar fields by solving numerically a Hamilton-Jacobi pde (cf. [33] for a different way of approaching a level-set construction). The main issue with these methods, in addition to the difficulty of harmonic functions to handle complex obstacle geometries, is related to the complexity of solving the associated PDE. In contrast, navigation functions admit analytic algebraic representations of the obstacles and there is a constructive way of generating them, but the majority of related work in this direction treats (simple) spherical obstacles [34]–[36]; see [37] for exceptions.

In the case of *dynamic environments*, the potential field landscape is different. Known heuristics are (re)introduced to tackle the time-varying nature of the workspace: virtual forces [38]—see [39], [40] for leader-following problems—which inevitably give rise to local minima [41], [42]; fuzzy logic [43], [44], or search-based methods [45], which come at the expense of completeness. Provably correct (local minima-free) potential fields have been constructed using fast marching methods [46] and sampling—computational complexity

issues here persisting—and with navigation functions on *sphere worlds only*, for the case of a moving destination [47]. Local potential-based methods [48], [49] have also tackled cases of moving destinations, but without consideration to collision avoidance. In related extensions that *do* account for obstacles [50], [51] and kinematic constraints, the environment is static.

This paper contributes by (a) reducing the algebraic complexity associated with workspace representation in navigation functions through a unified description of common obstacle classes, and mainly by (b) proving that, under some mild assumptions, the purging (Fig. 2) and star-to-sphere (Fig. 3b) transformations of the standard navigation function framework remain diffeomorphic when applied to the time-varying destination manifold case of [47], thereby extending the aforementioned approach to star worlds, including forests of stars.

Time-varying destination functions in sphere worlds [47] are first reviewed in §II, and together with some necessary notation, the new obstacle representation approach is introduced. In §III it is shown that the nature of critical points of time-varying navigation functions is preserved under diffeomorphisms, and this serves as the foundation for the transformations constructed later in the section. Testing and validation results are presented in §IV, first illustrating the application of transformations, and then offering both simulation and experimental results, the latter involving a differential-drive mobile robot. Conclusions close the paper in §VI.

II. Problem Statement

Consider an n-dimensional Euclidean space $\mathbb{E}^n$. and a bounded n-dimensional robot workspace $\mathcal{W} \subset \mathbb{E}^n$, populated by a finite number of obstacles $\mathcal{O}_j$, for $j \in \mathcal{I}$.

If all $\mathcal{O}_j$ are *star shaped* (see Fig. 3a), then $\mathcal{W}$ is a *star world* [2]. Obstacle $\mathcal{O}_j$ is (strictly) *star shaped* if the ray starting from a designated interior point q_j (the center) to any other exterior point intersects its boundary exactly once. If $\beta_j(q)$ is a (smooth) *implicit representation* of $\mathcal{O}_j$ [1], meaning $\mathcal{O}_j \triangleq \{q \in \mathcal{W} : \beta_i(q) \leq 0\}$, then for a constant $\Delta_j > 0$ it should be the case that $\nabla\beta_j(q) \cdot (q - q_j) \geq 2\Delta_j$, for all $q \in \partial\mathcal{O}_j$ [1]. The boundary of $\mathcal{W}$ is similarly defined as an (outer) obstacle $\mathcal{O}_0$, having its own implicit representation in the form of function β_0, so that $\mathcal{W} \triangleq \mathrm{E}^n - \mathcal{O}_0$.

In a star world, all boundaries are either those of stars, or of *star trees*. A *star tree* $\mathcal{T}_i$ is a finite union of stars arranged in the workspace in such a way that (i) whenever in the tree's underlying partial order $\prec$ one finds that for two stars $\mathcal{O}_j \prec \mathcal{O}_m$ there is no $\mathcal{O}_k$ satisfying $\mathcal{O}_j \prec \mathcal{O}_k \prec \mathcal{O}_m$ (this property is denoted here $\mathcal{O}_j \preceq \mathcal{O}_m$) this fact implies that the center of $\mathcal{O}_m$ is an interior point of $\mathcal{O}_j$; and (ii) for any $\mathcal{O}_j$ in the tree, there is only one $\mathcal{O}_j$ such that $\mathcal{O}_j \preceq \mathcal{O}_m$. Thus a tree is a group of stars that are partially overlapping and can admit a partial

order which essentially expresses an ancestor-descendant relationship between them. If $\mathcal{O}_j \preceq \mathcal{O}_m$, then $\mathcal{O}_j$ is called the *parent* of $\mathcal{O}_m$ and is equivalently denoted $\mathcal{O}_{p_m}$.

A *forest of stars* is a finite union of star trees. Assume that there are M trees in $\mathcal{W}$, and denote q_i the center of the *root* star in tree $\mathcal{T}_i$. The robot's *free space* is denoted $\mathcal{F} \triangleq \mathcal{W} - \bigcup_{i=1}^{M} \mathcal{T}_i$, and it is assumed to be path-connected.

There are two main characteristics that distinguish the time-varying navigation functions here (cf. [47]) and those of the traditional formulation [2]: (i) the destination coordinates x_t are time-varying, and (ii) there is a spherical "protective bubble" $\mathcal{B}_r^{x_t}$ of radius r around x_t to ensure a safe minimal distance between robot and target. Similarly, obstacle (star) trees are not allowed to intersect with each other or with $\mathcal{B}_r^{x_t}$.

The robot is required to converge on the surface of $\mathcal{B}_r^{x_t}$. Inside $\mathcal{F}$, a *time-varying navigation function* is defined.

Definition 1. *Given a free space $\mathcal{F}$ and a sphere $\mathcal{B}_r^{x_t}$ of radius r centered at a time-varying point x_t, a map $\varphi: \mathcal{F} \to [0,1]$ is a time-varying navigation function if it satisfies the following conditions: 1) It is a $C^{(2)}$ function on $\mathcal{F}$; 2) it has a uniform value on the boundary of $\mathcal{F}$ (admissible); 3) the nowhere dense*[1] *set $\partial\mathcal{B}_r^{x_t}$ is the only attractive manifold in $\mathcal{F}$.*

A. Time-varying navigation functions in sphere worlds

A *sphere world* is a subset of $\mathbb{E}^n$, where all objects of interest are spherical. The sphere world has a (spherical) boundary, which is at a constant distance ρ_0 from a point x_0. The interior of the sphere world workspace is the complement of $\mathring{\mathcal{O}}_0 \triangleq \{x \in \mathbb{E}^n : \| x - x_0 \| \geq \rho_0\}$. Inside this sphere world there can be M (spherical) obstacle regions $\mathring{\mathcal{O}}_i$, each with radius ρ_i, $i = 1, \ldots, M$, having implicit representations $\mathring{\beta}_i(x) = \| x - x_i \|^2 - \rho_i^2$. The *free sphere-world space* is then $\mathcal{M} \triangleq \mathbb{E}^n - \bigcup_{i=0}^{M} \mathring{\mathcal{O}}_i$. Let $x_t \in \mathbb{E}^n$ be the position of a moving target, and r be a constant associated with the smallest distance that should be kept in relation to this target. Define the sphere-world *time-varying destination function* [47] as

$$\mathring{J}_r(x,t) \triangleq \left((\| x - x_t \|)^2 - r^2 \right)^2 \quad (1)$$

[1] A set is nowhere dense if its closure has an empty interior.

For $\mathscr{M}$ to be a *valid* sphere world free space, the obstacles (including $\{x \in \mathscr{M} \mid \exists t > 0 : \mathring{J}_r(x,t) = 0\}$) must all be disjoint (cf [2]). Let now $\kappa > 0$ be a constant, denote $\mathring{\beta}(x) \triangleq \Pi_{i=0}^{M} \mathring{\beta}_i(x)$, and define

$$\mathring{\varphi}(x) \triangleq \frac{\mathring{J}_r(x,t)}{\left[\mathring{J}_r(x,t)^{\kappa} + \mathring{\beta}(x)\right]^{\frac{1}{\kappa}}} \quad (2)$$

The fact that (2) is consistent with Definition 1, with $\mathscr{M}$ as free space, has been established [47]; specifically, it was shown that for $\mathring{\mathscr{B}}_r^{x_t} = \{x \in \mathscr{M} : \| x - x_t \| \leq r\}$, it is true that (i) all critical points other than those on $\partial\mathring{\mathscr{B}}_r^{x_t}$ are either non-degenerate with attraction regions of measure zero, or in the interior of $\mathring{\mathscr{B}}_r^{x_t}$, namely $\mathrm{int}\mathring{\mathscr{B}}_r^{x_t}$, and that (ii) $\partial\mathring{\mathscr{B}}_r^{x_t}$ is the only limit set of the gradient field $-\nabla\varphi$ with non-zero measure attraction region outside $\mathring{\mathscr{B}}_r^{x_t}$.

The problem treated in this paper is showing that the aforementioned properties are invariant under diffeormorphisms, meaning that (2) is a time-varying navigation function when $\mathscr{F}$ is a *star world*. The solution to the aforementioned problem is presented in §III. Before we do so, however, let us elaborate on how a star world $\mathscr{F}$ involving rectangular or cylindrical stars can be modeled efficiently.

B. Environment Modeling

The shape of a large class of obstacles in man-made environments can be adequately approximated by trees of rectangular solids, cylinders, and spheres. In the original formulation [1] such obstacles would be modeled in the form of finite Boolean combinations of linear and quadratic inequalities, and it has been shown that these constructions lend themselves to the definition of diffeomorphic transformations in $\mathscr{F}$. It turns out that these Boolean combinations are only one option; implicit obstacle representations that may be more analytically and computationally expedient can also be used.

There exists an analytic implicit representation of a twodimensional shape that "interpolates" smoothly between a circle and a square: the *Fernandez-Guastis Squircle* [52]. The use of the original squircle implicit representation in navigation functions, however, is problematic (creates spurious zero level sets) and a modified version is thus introduced here:

Definition 2 (cf. [52]). *The unit squircle in* $\mathbb{E}^2$ *is the zero level set of the function*

$$\beta_{\mathrm{sc}}(x,y) \triangleq \frac{x^2 + y^2 + \sqrt{x^4 + y^4 + (2 - 4s^2)x^2y^2}}{2} - 1 \quad (3)$$

where $s \in (0, 1)$ *is a constant parameter.*

Proposition 1. $\beta_{sc}(q)$ *is smooth in* $\mathbb{R}^2 - \{0\}$.

Proof: Note that the only potentially problematic term in terms of continuity for derivatives is the square root (at the origin). With $0 < s < 1$, and away from the origin, which is the center of the shape, we have $x^4 + y^4 + (2 - 4s^2)x^2y^2 > (x^2 - y^2)^2 \geq 0$. Thus, the term inside the square root is positive definite. ■

The following equivalent representation of β_{sc}, in which the argument is in vector form, is particularly convenient for calculating the length of rays from its center to its boundary. Denoting b_1 and b_2 any two base vectors in $\mathbb{E}^2$, and considering a point along the direction of a unit vector $\hat{q}$ at a distance r from the squircle's center, (3) becomes

$$\beta_{sc}(r, \hat{q}) = r^2 \frac{1 + \sqrt{1 - 4s^2[(\hat{q} \cdot b_1)(\hat{q} \cdot b_2)]^2}}{2} - 1 \quad (4)$$

Letting $\beta_2 = 0$, the length ρ_2 of the ray from center to the boundary of the unit squircle can be given as

$$\rho_{sc}(\hat{q}) = \sqrt{\frac{2}{1 + \sqrt{1 - 4s^2[(\hat{q} \cdot b_1)(\hat{q} \cdot b_2)]^2}}} \quad (5)$$

Based on an iterative process, the implicit representations (4) and the length of rays (5) of 2D unit squircles can be extended into n-dimensional spaces [53].

More general rectangular obstacles can be modeled through a process of rotation, translation and scaling. Given a scaling matrix $\mathrm{A} \in \mathbb{R}^{n \times n}$, a rotation matrix $\mathrm{R} \in \mathbb{R}^{n \times n}$, and a translation vector $l \in \mathbb{R}^n$, the implicit representation β of an n dimensional rectangular obstacles in $\mathbb{E}^n$ can be obtained by the coordinate transformation, $q = \mathrm{A}^{-1}\mathrm{R}^{-1}(q' - l)$, where q' is the vector of new coordinates. Note that rotations and translations do not change the expression of the length of rays for a unit squircle. For scaling, however, the expression of ray length naturally depends on the scaling parameter. Based on (5), the length of rays of a scaled unit squircle is given as $\rho(\hat{q}) = \| \mathrm{A}q' \| \rho_{sc}\left(\frac{\mathrm{A}^{-1}\hat{q}}{\| \mathrm{A}^{-1}\hat{q} \|}\right)$. In higher-dimensional cases, the above expression applies uniformly.

As a means of comparison, the case of a four-sided, twodimensional polygon modeled using the original [2] semi-algebraic construction would require the equivalent of 48 additions, 11 multiplications, and 28 exponentiations. To model the same object using squircles, one needs the equivalent of 6 additions, 5 multiplications, and 9 exponentiations.

III. Time-Varying Navigation Functions

This section shows that the properties of time-varying navigation functions in sphere worlds are preserved under star-to-sphere and purging transformations when the destination configuration is changing over time. Specifically, it is shown that under certain topological conditions, the transformations can remain diffeomorphic. Then, the properties of sphere-world time-varying navigation functions [47] are preserved.

A. Invariance Under Time-varying Diffeomorphisms

To prove that the properties of the star-world time-varying navigation functions are preserved under the new star-to-sphere and purging transformations [54], the following properties need to be established: (i) the transformations result in a bijection between the critical points of sphere-world and star-world navigation functions; (ii) the nature of the critical points related through this bijection is identical; and (iii) with the natural Euclidean topology of sphere-world and star-world spaces, the membership of critical points in the subsets of points “inside the destination bubble” and “close to obstacle boundaries” remains unaltered. The first assertion is established by examining the Jacobian of the transformation, while the second involves its Hessian.

Proposition 2 (cf. [54, Proposition 2.6]). *Let $\mathring{\varphi}(x)$ be a sphere-world navigation function* (2) *defined on $\mathcal{M}$, and $h:\mathcal{F}\to\mathcal{M}$ be a diffeomorphism from star-world $\mathcal{F}$ to sphere world $\mathcal{M}$. Let $\mathcal{B}_r^{x_t} \triangleq \{q:\ \| h(q)-x_t\|^2 \le r^2\}$, and denote $\mathrm{int}\mathcal{B}_r^{x_t}$ its interior. Then all the critical points of*

$$\varphi(q) \triangleq (\mathring{\varphi}\circ h)(q) \quad (6)$$

other than those on $\partial\mathcal{B}_r^{x_t}$, are either non-degenerate with attraction regions of measure zero, or in $\mathrm{int}\mathcal{B}_r^{x_t}$. In addition, the flows of $-\nabla\varphi$ have $\partial\mathcal{B}_r^{x_t}$ as the only limit set with non-zero measure attraction region outside $\mathrm{int}\mathcal{B}_r^{x_t}$.

Proof: Follows from the three following Lemmas.

Lemma 1 (cf. [54, Proof of Proposition 2.6]). *Let $\mathcal{C}_\varphi \triangleq \{q:\nabla\varphi(q)=0\}$ be the set of critical points of φ, and $\mathcal{C}_{\mathring{\varphi}} \triangleq \{x:\nabla\mathring{\varphi}(x)=0\}$ the set of critical points of $\mathring{\varphi}$. The restriction of h on $\mathcal{C}_\varphi$, denoted $\hat{h}:\mathcal{C}_\varphi\to\mathcal{C}_{\mathring{\varphi}}$, is bijective.*

Proof. Take $c\in\mathcal{C}_\varphi$ and denote D_h the Jacobian of h. The chain rule requires that $\nabla\varphi(c)=\nabla(\mathring{\varphi}\circ h)(c)=\mathrm{D}_h\big|_c^{\mathsf{T}}\nabla\mathring{\varphi}(h(c))$. Since h is a diffeomorphism, D_h is nonsingular, and thus it must be $c_0=h(c)\in\mathcal{C}_{\mathring{\varphi}}$. Given that h is injective, $\hat{h}$ must be bijective.

Lemma 2 (cf. [54, proof of Proposition 2.6]). *If* $c = h^{-1}(c_0) \in \mathscr{C}_\varphi$ *is a degenerate critical point, a local minimum, a local maximum or a saddle of* φ*, then* $c_0 \in \mathscr{C}_{\mathring{\varphi}}$ *is also a degenerate critical point, a local minimum, a local maximum or a saddle of* $\mathring{\varphi}$*, respectively.*

Proof. Let $u = h(q)$ for $x \in \mathscr{F}$. From the multivariate version of Faà di Bruno's formula [55], [56], for the Hessian $\mathrm{H}_\varphi \equiv \left[(\mathrm{H}_\varphi)_{ij}\right]$, evaluated at a critical point $q = c \in \mathscr{C}_\varphi$:

$$\mathrm{H}_\varphi\Big|_c = \left(\mathrm{D}_h^{\mathrm{T}}\mathrm{H}_{\mathring{\varphi}\circ h}\mathrm{D}_h + \sum_{k=1}^{n}[(\nabla\mathring{\varphi})_k \circ h]\mathrm{H}_{(h)_k}\right)|_c$$

Because $h(c) = c_0 \in \mathscr{C}_{\mathring{\varphi}}$ (Lemma 1), the second term of $\mathrm{H}_\varphi\big|_{c_0}$ vanishes, which implies $\mathrm{H}_\varphi\big|_c = \mathrm{J}_h^{\mathrm{T}}\big|_c \mathrm{H}_{\mathring{\varphi}}\big|_{h(c)} \mathrm{J}_h\big|_c$. Given that h is a diffeomorphism, $\mathrm{H}_{\mathring{\varphi}}\big|_{c_0}$ and $\mathrm{H}_\varphi\big|_c$ have the same rank and eigenvalues. □

Lemma 3. *For* $c \in \mathscr{C}_\varphi$*: (i) if* $c \in \partial\mathscr{B}_r^{x_t}$*, then* $h(c) \in \partial\mathring{\mathscr{B}}_r^{x_t}$*; (ii) if* $c \in \mathrm{int}\mathscr{B}_r^{x_t}$*, then* $h(c) \in \mathrm{int}\mathring{\mathscr{B}}_r^{x_t}$*; (iii) if* $c \notin \mathrm{cl}\mathscr{B}_r^{x_t}$*,* (cl *denoting closure) then* $h(c) \notin \mathrm{cl}\mathring{\mathscr{B}}_r^{x_t}$.

Proof. Straightforward: for critical point $c \in \mathscr{C}_\varphi$, and for each one of the cases identified above, (i) $c \in \partial\mathscr{B}_r^{x_t} \Leftrightarrow \| h(c) - x_t \|^2 = r^2 \Leftrightarrow h(c) \in \partial\mathring{\mathscr{B}}_r^{x_t}$; (ii) $c \in \mathrm{int}\mathscr{B}_r^{x_t} \Leftrightarrow \| h(c) - x_t \|^2 < r^2 \Leftrightarrow h(c) \in \mathrm{int}\mathring{\mathscr{B}}_r^{x_t}$; (iii) $c \notin \mathrm{cl}\mathscr{B}_r^{x_t} \Leftrightarrow \| h(c) - x_t \|^2 > r^2 \Leftrightarrow h(c) \notin \mathrm{cl}\mathring{\mathscr{B}}_r^{x_t}$. □ ■

B. Construction of Star-to-Sphere Transformations

For a star-shaped obstacle $\mathscr{O}_i$ with center q_i for $i \in \{1, \ldots, M\}$, let $\mathscr{O}_i(\epsilon) \triangleq \{q \in \mathscr{F} : \beta(q) \leq \epsilon\}$, where ϵ is a sufficiently small positive constant so that $\mathscr{O}_i(\epsilon) \subset \mathscr{F} \cup \partial\mathscr{O}_i$. It has been shown [1] that $\mathscr{O}_i(\epsilon)$ is also star-shaped, and it also satisfies $\nabla\beta \cdot (q - q_i) > 0$.

Stars are transformed into spheres by scaling their rays. The *scaling factors* are functions $v_i : \mathscr{F} \to \mathbb{R}_+$ defined as follows,

$$v_i(q) \triangleq \rho_i \frac{1 + \beta_i(q)}{\| q - q_i \|} \quad v_0(q) \triangleq \rho_0 \frac{1 - \beta_0(q)}{\| q - q_0 \|} \qquad (7)$$

for $i \in \{1, \ldots, M\}$ with q_i the center of the star. Because the scaling of one star in $\mathscr{F}$ should not interfere with that of another, these scalings are turned on and off by means of *analytical switches,* σ_i. After defining the *omitted product* of obstacle functions, $\bar{\beta}_i \triangleq \Pi_{j=0, j\neq i}\beta_j$, and

letting J_r express the destination manifold in $\mathcal{F}$ in a way analogous to (1), these analytical switches are parameterized by a positive constant Λ and expressed uniformly for $i \in \{0, \ldots, M\}$ as

$$\sigma_i(q,\lambda) \triangleq \frac{x}{x+\lambda} \circ \frac{J_r(q,t)\bar{\beta}_i(q)}{\beta_i(q)} = \frac{J_r(q,t)\bar{\beta}_i(q)}{J_r(q,t)\bar{\beta}_i(q) + \lambda\beta_i(q)}$$

Assume now that the constructed star world $\mathcal{F}$ and its model sphere world $\mathcal{M}$ satisfy two constraints, referred to as the *placement condition* and the *containment condition*:

Assumption 1. *For $i = \{0, \ldots, M\}$, denote $q_i \in \mathcal{F}$ and $x_i \in \mathcal{M}$ the obstacle centers in star world $\mathcal{F}$ and model sphere world $\mathcal{M}$, and let J_r express the destination manifold in $\mathcal{F}$. Star world $\mathcal{F}$ and sphere world $\mathcal{M}$ satisfy*

- *the* placement condition *if $\forall i \in \{0, \ldots, M\}$ it is $x_i = q_i$, and $\forall x \in \mathcal{M}$, $q \in \mathcal{F}$ one has $\mathring{J}_r(x,t) \equiv J_r(q,t)$, and*
- *the* containment condition *if $\forall q \in \mathcal{O}_i(\epsilon)$, $i \in \{1, \ldots, M\}$ it is $v_i(q) \leq 1$, and $\forall q \in \mathcal{O}_0(\epsilon)$ it holds that $v_0(q) \geq 1$.*

Once this assumption is in place, the transformation that maps a star-world $\mathcal{F}$ to a sphere-world $\mathcal{M}$ can be defined.

Definition 3. *The star world to sphere world transformation, $h_\lambda : \mathcal{F} \to \mathcal{M}$, with $\sigma_d \triangleq 1 - \Sigma_{i=0}^{M} \sigma_i$, is defined as*

$$h_\lambda(q) \triangleq \sum_{i=0}^{M} \sigma_i(q,\lambda)[v_i(q) \cdot (q - q_i) + p_i] + \sigma_d(q,\lambda)q \quad (8)$$

It should be stressed that contrary to the original definition [1], (8) is *time-varying* because σ_i are. That (8) defines a diffeomorphic mapping has not been established, but Theorem 1 that follows does exactly that; cf. [1, Theorem 6].

Theorem 1. *For any star world $\mathcal{F}$, there exists a suitable sphere world $\mathcal{M}$ and a positive constant Λ, such that if $\lambda \geq \Lambda$, then $h_\lambda : \mathcal{F} \to \mathcal{M}$ is a diffeomorphism.*

Proof. The process of proving that (8) is a diffeomorphism rests on [1, Proposition 4.4.3], which states three conditions for it to first be a homeomorphism; then, given that h_λ is analytic and has a nonsingular Jacobian, and together with being one-on-one on $\mathcal{F}$, the fact that h_λ is a diffeomorphism follows directly from the Inverse Function Theorem. In this proposition $\mathcal{X}$ and $\mathcal{Y}$ are to be understood as n-dimensional continuously differentiable compact connected manifolds with $M + 1$ disjoint boundary components. Denote $\partial\mathcal{X}_j$ and $\partial\mathcal{Y}_j$ their jth boundary component, and let each be a compact $(n-1)$-dimensional connected manifold. For h_λ now to be a homeomorphism, (i) h_λ should have a nonsingular Jacobian,

(ii) its restriction on $\partial\mathcal{X}_j$ should be a bijection onto $\partial\mathcal{Y}_j$ for all obstacles $j = 0, \ldots, M$, and (iii) it should map neighborhoods of $\partial\mathcal{X}_j$ onto neighborhoods of $\partial\mathcal{Y}_j$. The process of establishing the nonsingularity of the Jacobian of h_λ, denoted D_{h_λ}, involves three steps, each established by a corresponding lemma. Each lemma establishes the behavior of the Jacobian in a particular region of $\mathcal{F}$.

With reference to an obstacle's center q_i, the tangent space $T_q\mathcal{F}$ of $\mathcal{F}$ at q can be expressed as the direct sum of two subspaces in the form $T_q\mathcal{F} = \mathrm{span}\{q - q_i\} \oplus \mathrm{span}\{q - q_i\}^\perp$. Thus any vector $y \in T_q\mathcal{F}$ can be uniquely expressed by two components y_1 and y_2 in each orthogonal subspace, that is, $y = y_1 + y_2$ with $y_1 \in \mathrm{span}\{q - q_i\}$ and $y_2 \in \mathrm{span}\{q - q_i\}^\perp$. Now consider a unit sphere $S_q^n \in T_q\mathcal{F}$ centered at q, and denote $\hat{u}$ the unit vector along the direction of any $u \in T_q\mathcal{F}$. Given a parameter $\epsilon > 0$, $\mathcal{F}$ is partitioned into

- the *set away from obstacles* $\mathcal{A}(\epsilon) \triangleq \{q \in \mathcal{F} : \beta_0(q) \geq \epsilon \wedge \cdots \wedge \beta_M(q) \geq \epsilon\}$, and
- a collection of obstacle neighborhood sets, $\{\mathcal{O}_i(\epsilon)\}_{i=0}^M$.

For the latter, the analysis of the behavior of D_h considers two cases: along (unit) directions within, and outside, the cone

$$C_q \triangleq \left\{ y \in S_q^n : \frac{\| y_1 \|}{\| y_2 \|} > \sqrt{2}[\widehat{\nabla\beta_i} \cdot (\widehat{q - q_i})]^{-1} \right\} \quad (9)$$

The Jacobian can be made nonsingular on $\mathcal{A}(\epsilon)$ if λ is picked sufficiently large; the proof is in the Appendix:

Lemma 4. *There exists* $\Lambda_0(\epsilon) > 0$, $\forall \epsilon > 0$, *such that if* $\lambda \geq \Lambda_0$, *the Jacobian* D_{h_λ} *of* h_λ *is non-singular on* $\mathcal{A}(\epsilon)$.

Similarly, for each $\mathcal{O}_i(\epsilon)$, as long as the ray near the boundary points "outwards" (which is true for star-shaped obstacles), there are no zero eigenvalues associated with eigenvectors along directions in C_q; the proof is in the Appendix:

Lemma 5. *Let* ϵ_{i0} *be a positive constant such that* $\nabla\beta_i \cdot (q - q_i) > 0$ $\forall q \in \mathcal{O}_i(\epsilon_{i0})$. *There exist*[2] *two constants,* $\epsilon_{i1} < \epsilon_{i0}$ *and* Λ_{i1}, *such that for all* $\epsilon < \epsilon_{i1}$, *and* $q \in \mathcal{O}_i(\epsilon)$, *if* $\lambda > \Lambda_{i1}(\epsilon)$, *then* $\hat{y}^{\mathrm{T}} D_{h_\lambda}(q)\hat{y} > 0$, $\forall \hat{y} \in C_q$.

And finally, the quadratic forms above can be made strictly positive in $\mathcal{O}_i(\epsilon)$ for directions *outside* C_q; the proof is in the Appendix:

[2] ϵ_{i0} exists because β_i is a continuous implicit representation of a strict star.

Lemma 6. *Let ϵ_{i0} be a positive constant such that $\nabla\beta_i \cdot (q - q_i) > 0\ \forall q \in \mathcal{O}_i(\epsilon_{i0})$. There exist constants $\epsilon_{i2} < \epsilon_{i0}$ and Λ_{i2}, such that for all $\epsilon < \epsilon_{i2}$, $\forall q \in \mathcal{O}_i(\epsilon)$, if $\lambda > \Lambda_{i2}(\epsilon)$, then $\forall \hat{y} \in S_q^n - C_q$ and $\forall \hat{y}_2 \in \text{span}\{q - q_i\}^{\perp}$, $\hat{y}_2^{\mathrm{T}} \mathrm{D} h_\lambda(q) \hat{y} > 0$.*

By combining now Lemmas 4 through 6, one can choose $\epsilon < \epsilon_i \triangleq \min\{\epsilon_{i1}, \epsilon_{i2}\}$ and $\lambda > \Lambda_i(\epsilon) \triangleq \max\{\Lambda_{i1}, \Lambda_{i2}\}$, and then pick a single ϵ^* and λ^* as follows:

$$\epsilon^* \triangleq \min_{j \in \{0, \ldots, M\}} \{\epsilon_j\} \quad \lambda^* \geq \max_{j \in \{0, \ldots, M\}} \{\Lambda_j(\epsilon^*)\} \qquad (10)$$

To see now that h_λ maps the boundary of star i, $\partial\mathcal{O}_i$, to the boundary of sphere i, $\partial\mathring{\mathcal{O}}_i$, let $q \in \partial\mathcal{O}_i$; then by the construction, $\beta_i(q) = 0$ and $\beta_j(q) > 0$ for any $j \neq i$. Therefore, $h_\lambda \Big|_{\partial\mathcal{O}_i} = \frac{\rho_i}{\| q - q_i \|}(q - q_i) + p_i$, which means that $h_\lambda(q)$ for $q \in \partial\mathcal{O}_i$ is at a distance ρ_i from the center p_i of sphere obstacle $\mathring{\mathcal{O}}_i$. Thus, $h_\lambda(\partial\mathcal{O}_i) \subseteq \partial\mathring{\mathcal{O}}_i$, for $i \in \{0, \ldots, M\}$. In addition, $h_\lambda \big|_{\partial\mathcal{O}_i}$ is injective; this can be shown by contradiction: assume otherwise, which implies the existence of two points q and q', both in $\in \partial\mathcal{O}_i$, such that $\frac{\rho_i}{\| q - q_i \|}(q - q_i) + p_i = \frac{\rho_i}{\| q' - q_i \|}(q' - q_i) + p_i, \Leftrightarrow \| q' - q_i \| (q - q_i) = \| q - q_i \| (q' - q_i)$, and in turns suggests that points $(q - q_i)$ and $(q' - q_i)$ are on the same ray. But this is impossible since they are on the boundary of a star. The proof that $h_\lambda \big|_{\partial\mathcal{O}_i}$ is surjective follows the same procedure as in [1, Theorem 6].

The last condition involves the mapping of neighborhoods. Take $q \in \partial\mathcal{O}_i$, consider the ray that starts from q_i and goes through q $r_q(s) \triangleq s(q - q_i) + q_i$ for $s \geq 0$. Note that $r_q(1) = q$. Then, using Lemma 5, since $(q - q_i)$ is in C_q, verify that:

$$\frac{\mathrm{d}\mathring{\beta}_i \circ h_\lambda \circ r_q}{\mathrm{d}s}\Big|_{s=1} = \frac{2\rho_i (q - q_i)^{\mathrm{T}} \mathrm{D} h_\lambda (q - q_i)}{\| q - q_i \|}\Big|_{q \in \partial\mathcal{F}_i} > 0$$

Given monotonicity, continuity, and that $(h_\lambda \circ r_q)(1) \in \partial\mathring{\mathcal{O}}_i$ implying that $(\mathring{\beta}_i \circ h_\lambda \circ r_q)(s)\big|_{s=1} = 0$, there should be some s' such that $(\mathring{\beta}_i \circ h_\lambda \circ r_q)(s)\big|_{s=1} > 0$ for $s \in (1, 1 + s')$. With $\partial\mathcal{O}_i$ compact, there is a lower bound $s_0 < s'$ over the whole obstacle boundary, that guarantees that $(\mathring{\beta}_i \circ h_\lambda \circ r_q)(s)\big|_{s=1} > 0$ for all $q \in \partial\mathcal{O}_i$ as long as $s \in (1, 1 + s_0)$. □

C. Construction of time-varying purging transformations

The time-varying purging transformation introduced in this section is an extension of Rimon's original constructions [1]: unlike the original purging transformation, which only deals with planar and parabolic obstacles, the transformations here apply to any star-shaped obstacle for which the implicit representation and length of rays are known.

Any star tree $\mathcal{T}_j$ has a nonempty set of *leaves*, that is, stars $\mathcal{O}_i \in \mathcal{T}_j$ which are the minimal elements in the tree's partial order—meaning that there is no $\mathcal{O}_k \in \mathcal{T}_j$ such that $\mathcal{O}_i \preceq \mathcal{O}_k$. The set of leaves of all trees in workspace $\mathcal{W}$, is denoted $\mathcal{L}$. Every obstacle, including the leaves, is connected to its unique parent via a surface called the *patch* $\mathcal{P}_{p_i} \triangleq \mathcal{O}_i \bigcap \partial \mathcal{O}_{p_i}$. Unlike traditional purging transformations [2], here $\mathcal{P}_{p_i}$ does not need to be simply connected. The purpose of the purging transformation is to reduce the leaves to their corresponding patches, transforming $\mathcal{F}$ to the *purged* free space $\widehat{\mathcal{F}} \triangleq \mathcal{F} \bigcup_{i \in \mathcal{L}} (\mathcal{O}_i - \mathcal{O}_{p_i})$. The process is repeated until there are no leaves left, and trees of stars are reduced to their root star obstacles.

Without significant loss of generality (the center of a star is not unique) it is assumed that at each iteration of the purging transformation the centers of parent and leaf stars are picked so that they coincide. (Subsequent applications can use different centers.) Denote that common center $p_i \in \mathcal{O}_i \bigcap \mathcal{O}_{p_i}$. The geometric constants introduced in the following definition are used to describe a "collar" on the boundary of the parent, where it intersects with its child.

Definition 4. *The positive constants E_i, E_d, are such that*

$$\mathcal{O}_i(2E_i) \bigcap \mathcal{O}_j(2E_j) = \varnothing \;\; \mathcal{B}^{x_t}_{r+E_d} \bigcap \mathcal{O}_j(2E_j) = \varnothing$$

for $i, j \in \mathcal{I}$ with $p_j \neq i \neq j \neq p_i$.

The scaling factors utilized in the purging transformation differ slightly from (7), by the introduction of the scalar

$$\widetilde{\kappa}_i(q) \triangleq \beta_{p_i}(q) + \beta_i(q) - 2E_i + \sqrt{\beta^2_{p_i}(q) + (\beta_i(q) - 2E_i)^2}$$

and with $\rho_{Pi}(q)$ denoting the length of rays from center to boundary of the parents of leaf i, the purging transformation scaling maps of $i \in \mathcal{L}$ are expressed as $v_i(q) \triangleq \rho_{p_i}(q) \frac{1 + \beta_i(q)\widetilde{\kappa}_i(q)}{\| q - q_i \|}$.

Those ray lengths ρ_{P_I} are assumed to be *properly bounded*, meaning that they should have a lower bound $\rho_{\min}$ in $\mathcal{O}_i(\epsilon)$, and an upper bound $\rho_{\max}$ in $\mathcal{F}$.

Once the scaling factors are in place, the maps f_i that scale the rays from the center p_i of each leaf, for $i \in \mathcal{L}$ are expressed in the form of $f_i(q) \triangleq v_i(q)(q - q_i) + p_i$.

To construct the *analytic switches* of the purging transformation, which blend together the scaling maps, first define

$$\tilde{\beta}_i \triangleq \beta_{p_i}(q) + 2E_i - \beta_i(q) + \sqrt{\beta_{p_i}^2(q) + (\beta_i(q) - 2E_i)^2}$$

and modify the expression for the *omitted product* as

$$\bar{\beta}_i \triangleq J_r(q,t)\left(\prod_{k \in \mathcal{I} - \{i, p_i\}} \beta_k\right)\left(\prod_{k \in \mathcal{L} - \{i\}} \beta_k\right)$$

form the analytic switches of the purging transformation, for $i \in \mathcal{L}$, as

$$\sigma_i(q,\mu) \triangleq \left(\frac{q}{q+\mu}\right) \circ \left(\frac{\bar{\beta}_i \tilde{\beta}_i}{\beta_i}\right) = \frac{\bar{\beta}_i \tilde{\beta}_i}{\bar{\beta}_i \tilde{\beta}_i + \mu \beta_i}.$$

Definition 5. *Let $\mathcal{F}$ be a forest of stars. The purging transformation $f_\mu : \mathcal{F} \to \widehat{\mathcal{F}}$ is a continuous map defined as*

$$f_\mu(q) \triangleq \sum_{i \in \mathcal{L}} \sigma_i(q,\mu) f_i(q) + \sigma_d q \quad (11)$$

With $\sigma_d \triangleq 1 - \Sigma_{i \in \mathcal{L}} \sigma_i$.

The proof that this particular purging transformation is a diffeomorphism is based on the following proposition.

Proposition 3 ([1, Proposition 4.4]). *Let $\mathcal{C} \subset \partial\mathcal{X}$ be closed and nowhere dense in $\partial\mathcal{X}$. A continuous map $h : \mathcal{X} - \mathcal{C} \to \mathbb{E}^n$ of class $C^{(q)}$ where $q \geq 1$, is a homeomorphism onto $\mathcal{Y}$ if*

1) *h has a non-singular Jacobian on $\mathcal{X} - \mathcal{C}$;*
2) *$h \mid \partial_j \mathcal{X}$ is a bijection onto $\partial_j \mathcal{Y}$ for $j = 0, \ldots, M$.*

Based on the above proposition, the following theorem establishes the nature of the purging transformation (11); cf. [1, Theorem 7].

Theorem 2. *For any forest of stars $\mathcal{F}$ and its purged version $\widehat{\mathcal{F}}$, there exists a positive constant Λ, such that if $\mu \geq \Lambda$, then $f_\mu : \mathcal{F} \to \widehat{\mathcal{F}}$ is a diffeomorphism.*

Proof. In general, the workspace boundary ∂F contains a nowhere dense set $\mathcal{S}$ of such *sharp corners*, particularly where a parent star $\mathcal{O}_{p_i}$ is joined with its child $\mathcal{O}_i$. Specifically in this region, and due to the introduction of the $2E_i$ "collar" around $\mathcal{O}_i$ (see [2, Fig. 9]), there are two neighboring areas of $\partial\mathcal{F}$ where one finds sharp corners: (i) the intersection of the leaves' boundary and their parents' boundary $\mathcal{S}_1 \triangleq \bigcup_{i \in \mathcal{L}} \partial\mathcal{O}_i \bigcap \partial\mathcal{O}_{p_i}$, and (ii) the intersection of the

parents' boundary with the "$2E_i$ thickened" version of the leaves, $\mathcal{S}_2 \triangleq \bigcup_{i \in \mathcal{L}} \mathcal{O}_i(2E_i) \bigcap \partial \mathcal{O}_{p_i}$. Thus, $\mathcal{S} \triangleq \mathcal{S}_1 \cup \mathcal{S}_2$. It is also the case that for the collar region on the parent's p_i boundary it holds that $\nabla \beta_i \cdot (q - q_i) \geq \Delta_i, \forall q \in \mathcal{O}_i(E_i) - \mathcal{S}$. Similarly to Theorem 1, showing that f_μ is a homeomorphism consists of three parts: (i) f_μ has a nonsingular Jacobian, (ii) f_μ is a bijection on the boundary, and (iii) it maps local neighborhoods of the boundary of a leaf to local neighborhoods for the "seam" between itself and its parent.

Take $\epsilon > 0$ and denote $\mathcal{A}_{\mathcal{L}} \triangleq \bigcup_{i \in \mathcal{L}} \{q \in \mathcal{F} \mid \beta_i(q) > \epsilon\}$, the free-space region ϵ–away from leaves. The Jacobian D_{f_μ} of f_μ is nonsingular on $\mathcal{A}_{\mathcal{L}}(\epsilon) - \mathcal{S}$, that is, away from leaves and boundary locations with sharp corners:

Lemma 7. *Given a forest of stars in* $\mathcal{F}$, *and for any* $\epsilon > 0$, *there exists a positive constant* $\Lambda_0(\epsilon)$, *such that if* $\mu \geq \Lambda_0(\epsilon)$, *then* D_{f_μ} *is nonsingular on* $\mathcal{A}_{\mathcal{L}}(\epsilon) - \mathcal{S}$.

The same holds true in the vicinity of obstacles, as long as sharp corners are avoided:

Lemma 8. *For every leaf* $i \in \mathcal{L}$ *in a star forest, there exist positive constants* ϵ_i *and* Λ_i, *such that if* $\mu \geq \Lambda_i$ *and* $\epsilon \leq \epsilon_i$, D_{f_μ} *is nonsingular on* $\mathcal{O}_i(\epsilon) - \mathcal{S}$.

The proof of Lemmas 7 and 8 are in the Appendix.

The nonsingularity of D_{f_μ} is now ascertained as follows. Pick $\epsilon^* \triangleq \min_{i \in \mathcal{L}} \epsilon_i$ and $\mu \geq \Lambda_1 \triangleq \max_{i \in \mathcal{L}} \Lambda_i$. Lemma 8 implies that D_{f_μ} is nonsingular on $\bigcup_{i \in \mathcal{L}} \mathcal{O}_i(\epsilon^*)$ less $\mathcal{S}$. If μ is further restricted so that $\mu \geq \max\{\Lambda_1, \Lambda_0 * (\epsilon^*)\}$, then D_{f_μ} is also nonsingular on $\mathcal{A}_{\mathcal{L}}(\epsilon^*)$ less $\mathcal{S}$. The conjunction of these two statements leaves D_{f_μ} nonsingular on $\mathcal{F} - \mathcal{S}$.

Let $q \in \partial \mathcal{O}_i$; then by construction, $\beta_i(q) = 0$ and $\beta_j(q) > 0$ for any $j \in \mathcal{L}$ and $i \neq j$. Therefore, $f_\mu \Big|_{\partial_i \mathcal{F} \bigcap \mathcal{F}} = \frac{\rho_{p_i}}{\| q - q_i \|}(q - q_i) + q_i$, which means that for $q \in \partial \mathcal{O}_i$, $f_\mu(q)$ is at distance ρ_{P_i} from the center q_i of the parent obstacle $\mathcal{O}_{p_i}$. Thus, $f_\mu(\partial \mathcal{O}_i) \subseteq \partial \mathcal{O}_{p_i}$, for $i \in \mathcal{L}$. In addition, $f_\mu \big|_{\partial \mathcal{O}_i}$ is injective; this can be seen by contradiction: if otherwise, then there would be two points q and q', both in $\in \partial \mathcal{O}_i$, such that

$$\frac{\rho_{p_i}}{\| q - q_i \|}(q - q_i) + q_i = \frac{\rho_{p_i}}{\| q' - q_i \|}(q' - q_i) + q_i \Leftrightarrow \| q' - q_i \| (q - q_i) = \| q - q_i \| (q' - q_i),$$

which in turns suggests that points $(q - q_i)$ and $(q' - q_i)$ are on the same ray. This is impossible: they are on the boundary of a star. The proof that $f_\mu \big|_{\partial \mathcal{O}_i}$ is surjective mirrors that of [1, Theorem 6] paraphrased as follows. If $\mu \geq \Lambda$, there exists an open neighborhood in $\mathcal{F}$ in which f_μ has a non-singular Jacobian, indicating that $f_\mu \big|_{\partial \mathcal{O}_i}$ is a local homeomorphism

(Inverse Function Theorem). A local homeomorphism from a compact space into a connected one, is surjective.

Take now $q \in \partial\mathcal{O}_i$, and consider the ray that starts from q_i and goes through q, $r_q(s) \triangleq s(q - q_i) + q_i$ for s ≥ 0. Then

$$\left.\frac{\mathrm{d}\beta_{p_i} \circ h_\lambda \circ r_q}{\mathrm{d}s}\right|_{s=1} = \left.\nabla\beta_{p_i}(q')^{\mathsf{T}}\right|_{q' \in \partial\mathcal{O}_{p_i}} \left.\mathrm{D}_{h_\lambda}(q - q_i)\right|_{q \in \partial\mathcal{F}_i}$$

For $\left.\nabla\beta_{p_i}(q')\right|_{q' \in \partial\mathcal{O}_{p_i}} \in \mathbb{R}^n$, one can show that it can always be decomposed into two vectors, q'_1 and q'_2, such that $q'_1 \in \mathrm{span}\{q - q_i\}$ and $q'_2 \in C_q \triangleq \{x \in T_q\mathcal{F}: \| x_2 \| \leq r_i \| x_1 \| \}$. The decomposition is done as follows: For all $x \in T_q\mathcal{F}$, $x = x_1 + x_2$ with $x_1 \in \mathrm{span}\{q - q_i\}$, and $x_2 \in \mathrm{span}\{q - q_i\}^\perp$. Given any cone C_q, there is a corresponding $r_i \in \mathbb{R}$, such that $x \in C_q$ if $\|x_2\| \leq r\|x_1\|$. To decompose now $\left.\nabla\beta_{p_i}(q')\right|_{q' \in \partial\mathcal{O}_{p_i}}$, first split $\left.\nabla\beta_{p_i}(q')\right|_{q' \in \partial\mathcal{O}_{p_i}}$ into components y_1 and y_2 along $\mathrm{span}\{q - q_i\}$ and $\mathrm{span}\{q - q_i\}^\perp$, respectively, so that $\left.\nabla\beta_{p_i}(q')\right|_{q' \in \partial\mathcal{O}_{p_i}} = y_1 + y_2$. Choosing $0 < r_0 < r$, let $y_3 = r_0 \| x_2 \| \widehat{(q - q_i)}$, and denote $q'_1 = y_1 - y_3$, $q'_2 = y_2 + y_3$. Then according to Lemma 9,

$$\left.\frac{\mathrm{d}\beta_{p_i} \circ h_\lambda \circ r_q}{\mathrm{d}s}\right|_{s=1} = q'^{\mathsf{T}}_1 \left.\mathrm{D}_{h_\lambda}(q - q_i)\right|_{q \in \partial\mathcal{F}_i} + q'^{\mathsf{T}}_2 \left.\mathrm{D}_{h_\lambda}(q - q_i)\right|_{q \in \partial\mathcal{F}_i} > 0 \quad (12)$$

Given that $(f_\mu \circ r_q)(1) \in \partial\beta_{p_i} \Rightarrow \left.(\beta_{p_i} \circ f_\mu \circ r_q)(s)\right|_{s=1} = 0$, in conjunction with continuity and monotonicity from (12), there exists s' such that $(\beta_{p_i} \circ f_\mu \circ r_q)(s)|_{s=1} > 0$ for some $s \in (1, 1 + s')$. Since $\partial\mathcal{O}_i$ is compact, there is a lower bound $s_0 < s'$ over the obstacle boundary, guaranteeing that $(\beta_{p_i} \circ h_\lambda \circ r_q)(s)|_{s=1} > 0$ for all $q \in \partial\mathcal{O}_i$ as long as $s \in (1, 1 + s_0)$. □

IV. Validation

This section illustrates the construction of two instances of environment representations, along with the time-varying navigation functions and the associated transformations. The two workspaces are of progressively higher complexity, with the first one containing two isolated obstacles, and the second one resembling a maze-like environment. The section couples these constructions with simulation studies with a point-mass robot, and experimental data obtained on a differential drive wheeled robot.

A. Workspace Modeling

The first case study attempts to model a small playground for children, mirroring the one utilized in a pediatric rehabilitation clinical study that motivates this work (see Fig. 4). The particular study involves games of chase between infants and robots, and the idea is to enable the robot to chase the human subject autonomously, using localization information provided through a system of networked cameras.

The general layout of this simple playground is shown in Fig. 5a. The outer square marks the outer boundary of the playground. The circle represents a round table-toy, where as the L-shaped obstacle is a combination of a foam ramp on one side and a small staircase (cf. Fig. 4). The L-shaped obstacle is thought of as a star tree, with $\mathcal{O}_1$ being the root, and $\mathcal{O}_2$ as the single leaf. In this case, the moving destination is the human subject.

If $\varphi_0(q)$ denotes the time-varying navigation function in the *sphere world,* $h(q)$ the star-to-sphere transformation, and $f(q)$ the purging transformation, then the time-varying navigation function $\varphi(q)$ for this workspace instance is given as $\varphi(q) = \varphi_0 \circ h \circ f(q)$. Assuming, without loss of generality, that the destination is momentarily at the geometric center of the workspace, the stages of the purging transformation that maps the star world to a sphere world are illustrated in Fig. 6.

The second case study emulates a maze-like environment, and is intended to highlight the application of the purging transformations. The environment layout in this case is shown in Fig. 5b (left). Here, all obstacles share a common ancestor: the outer workspace boundary. The long rectangular obstacles that represent walls are connected sequentially to form star trees, and to facilitate the application of purging transformations which would otherwise be challenging due to their elongated shape, *virtual* obstacles are used to patch the parent obstacle with its child (Fig. 5b (right)). This is done because when the center of the parent star does not coincide with its geometric center, straightforward application of (5) will introduce errors, since the latter is developed based on the geometric star (squircle) center. These (additional) virtual obstacles rectify this discrepancy and serve as links between parent and children stars, thus facilitating a sufficiently accurate approximation of the length of rays, needed for the purging transformations. In Fig. 5b, a purging transformation is applied four times consecutively, each time resulting in a transformed workspace depicted in the component figures of Fig. 7. Once all obstacles have been purged into the outer boundary, a star-to-sphere transformation maps to the sphere world of the bottom rightmost plot.

B. Simulation results

In this section, simulation results for an ideal point-mass robot are presented, ignoring any kinematic and dynamic constrains. The particular objective of the simulation study is to assess the capacity of the time-varying navigation function to offer target interception solutions. In every scenario, the robot is assumed to be able to develop speeds that exceed that of its target, to allow for interception. The radius of the bubble around the target is set at 0.1 m.

The first simulation result is presented in Fig. 8. The figure illustrates two scenarios of target motion. In the first (left), the target moves along a rounded square path tracing the outer boundary of the robot's workspace. The robot starts at coordinates (0, −1) m and chases the target as it goes around, "cutting the corners" to gain on it, and eventually intercepting it close to the lower right segment of the target's path. Below this picture of workspace and agent paths, the evolutions of the value of the navigation function, and that relative distance between target and robot, are plotted over time. Figure 9 offers snapshots at different time instances, indicating how the potential field changes as the target moves in this scenario. In the rightmost plot of Fig. 8, the target is moving along a straight diagonal line from northwest to southeast, while the robot starts at (−4, −4) m.

The first scenario illustrates a key feature of the approach. A navigation strategy based exclusively on the negated gradient of the time-varying navigation function *does not necessarily decrease monotonically* the value of the function. Depending on how the target moves, the relative distance between robot and target can fluctuate. This paper is not concerned with the stability properties of the relative distance dynamics and is part of future work. What this paper offers is illustrated better in Fig. 9. Under the stated conditions, the methodology presented *guarantees that for any fixed time, and irrespectively of the target's motion, φ is a navigation function*.

The second simulation study is conducted in a ROS/GAZEBO environment, where a quadrotor is steered in the 3d environment of Fig. 10 to intercept a moving target. In the environment of Fig. 10 the structures are being modeled as rectangular obstacles, in a conceptual 3d analog of the planar configuration depicted in Fig. 1.

C. Experimental results

This section reports experimental results from the application of the methodology on the small black differential-drive robotic toy shown in Fig. 4 (right). The control update frequency used was 10 Hz.

Two scenarios of leader-following were tested, and the results are shown in Fig. 11. Specifically, Fig. 11 presents snapshots from the two trials. In these trials, the target is another, remotely controlled, robot with differential drive kinematics, steered at a smaller speed than the pursuing robot. The snapshots from trial 1 depict the robot, initially in the upper left hand side corner of the workspace attempting to chase its target around the square obstacle that is between them. As the target moves from right to left south of the obstacle, the time-varying potential field readjusts and eventually directs the robot, straight down in pursuit of its target, rather than following the path of the target. In trial 2, the robot chases its target as it winds around the obstacles. A similarly interesting behavior resulting from the potential field appears in the last two snapshots (at 12 and 15 seconds) where the robot "waits" for its target to appear behind the obstacle, instead of just following its target's path.

V. Discussion

Before discussing advantages and limitations, it is important to frame this discussion relative to what the methodology actually offers. To iterate the last words of Section IV-B, the paper

claims that even when the destination configuration varies over time, the construction reported will offer a navigation function *for every time instant*. This is not the same as having a time-varying Lyapunov function for the kinematic system $\dot{x} = u$ under collision avoidance constraints. More work along is needed to establish the latter, but the methodology reported here is a big step in this direction.

With this clarified, let us review some advantages of the reported constructions. (a) In the case of dynamic environments, unlike heuristic approaches, the potential field generated by (6) does not have spurious attractors away from the destination manifold; (b) despite, again, the time-varying nature of the navigation scenario, collision avoidance is ensured globally, even without knowledge of the target's trajectory or enforcing visibility constraints; (c) no involved analytic integral calculations are required; (d) no configuration-space discretization is required, therefore circumventing complexity issues related to resolution and memory requirements; (e) due to the analytic nature of (6) bounded (kinematic) inputs are needed, under the assumption that the robot's maximum speed exceeds that of its target; (f) even for time-invariant cases, and compared with the original time-invariant construction [2] that utilizes Boolean combinations to represent semi-analytic obstacles, the reported method offers computational savings.

VI. Conclusion

The methodology of navigation functions on star worlds [2] can be extended to cases where the destination configuration is time-varying. The construction presented for this purpose in this paper preserves the main features of the classical approach, guaranteeing the absence of local minima when certain topological conditions are satisfied. Compared to earlier work along this direction which treated the case of sphere worlds with time-varying destinations [47], the present paper establishes the diffeomorphic nature of star-to-sphere and purging transformations, thus allowing the constructed potential fields to inherit the properties established in sphere worlds. In the process of reconstructing those transformations, novel, analytically and computationally expedient modeling formalisms were established for star-shaped obstacles. A new ROS toolkit is now publicly available for two-dimensional starshaped workspaces [57].

Acknowledgments

The authors sincerely thank Indrajeet Yadav for implementing and demonstrating their methodology in the GAZEBO environment of Fig. 10.

Portions of this work are supported by NIH R01HD87133 and HDTRA1-16-1-0039.

Appendix

Consider the vector $q_i - q$ with $q \notin \mathcal{S}$. The tangent space of $\mathcal{F}$ at q, $T_q\mathcal{F}$, can be expressed as the direct sum $T_q\mathcal{F} = \text{span}\{q_i - q\} \oplus \text{span}\{q_i - q\}^{\perp}$. Every $y \in T_q\mathcal{F}$ can be uniquely expressed as a sum of two components, one in each orthogonal subspace, such that $y = y_1 + y_2$, with $y_1 \in \text{span}\{q_i - q\}$, and $y_2 \in \text{span}\{q_i - q\}^{\perp}$. Denote $\hat{y}$ the unit vector along y.

A. Proof of Lemma 4

Let $\hat{y}$ be a unit vector at $q \in \mathscr{A}(\epsilon)$. Setting $w(\sigma_j, \nabla\sigma_j) \triangleq \Sigma_{j=0}^{M}\{\sigma_j(q-q_j)\nabla v_j^{\mathsf{T}} + (v_j-1)(q-q_j)\nabla\sigma_j^{\mathsf{T}}\}$ for brevity, one has [53, Lemma 4.5] $\mathrm{D}_{h_\lambda}\hat{y} = \left[1 - \Sigma_{j=0}^{M}\sigma_j(v_j-1)\right]\hat{y} + w(\sigma_j, \nabla\sigma_j)\hat{y}$. If $\lambda > \max_{j\in\{0,\ldots,M\}}\{N_{0j}(\epsilon,\delta), N_{1j}(\epsilon,\delta)\}$, then $\sigma_j(q,\lambda) < \delta$ and $\|\nabla\sigma_j(q,\lambda)\| \le \delta$ [53, Lemmas 4.6, 4.7]. Consequently, $\| w(\sigma_j, \nabla\sigma_j)\| < \delta\Sigma_{j=0}^{M}\| q-q_j\|(\|\nabla v_j\| + |v_j-1|)$. Note that $\delta_0' \triangleq \left[2\max_{\mathscr{A}(\epsilon)}\{\Sigma_{j=0}^{M}\| q-q_j\|\}(\|\nabla v_j\| + |v_j-1|)\right]^{-1}$ exists by continuity, and if $\delta \le \delta_0'$ then $\| w(\sigma_j, \nabla\sigma_j)\| < \frac{1}{2}$. Selecting δ, a bound for all σ_j with $j \in \{0, \ldots, M\}$ is established in $\mathscr{A}(\epsilon)$: $\sigma_j \le \left[2(1+M)\max_j\{|v_j-1|\}\right]^{-1}$, implying $1 - \Sigma_{j=0}^{M}\sigma_j(v_j-1) \ge \frac{1}{2}$. Define:

$$\delta_0 \triangleq \min_{j\in\{0,\ldots,M\}}\left\{\delta_0', [2(1+M)\max_j\{|v_j-1|\}]^{-1}\right\}$$

$$\Lambda_0(\epsilon) \triangleq \max_{j\in\{0,\ldots,M\}}\{N_{0j}(\epsilon,\delta_0), N_{1j}(\epsilon,\delta_0)\}$$

and select $\lambda \ge \Lambda_0$. Then $\mathrm{D}_{h_\lambda}\hat{y} \neq 0$. □

B. Proof of Lemma 5

$$\mathrm{D}_{h_\lambda}(q) = \underbrace{(q-q_i)(v_i-1)\nabla\sigma_i^{\mathsf{T}}}_{\mathrm{D}_{h1}(q,\lambda)} + \underbrace{\sum_{j=0, j\neq i}^{M}\{(v_j-1)\sigma_j\mathrm{I} + (q-q_i)[\sigma_j\nabla v_j + (v_j-1)\nabla\sigma_j]^{\mathsf{T}}\} + (1-\sigma_i+\sigma_i v_i)\mathrm{I} + (q-q_i)\sigma_i\nabla v_i^{\mathsf{T}}}_{\mathrm{D}_{h2}(q,\lambda)}$$

$\mathrm{D}_{h_1}(q,\lambda)$ is ensured positive semidefinite if

$$\beta_i \le \frac{(q-q_i)\cdot\nabla\beta_i}{6\| q-q_i\|\left[\Sigma_{j=0, j\neq i}^{M}\frac{\|\nabla\beta_j\|}{\beta_j} + 4\sqrt{\frac{\sqrt{J_r(q,t)}+r_t^2}{\sqrt{J_r(q,t)}}}\right]} \triangleq \zeta(q)$$

For $q \in \mathscr{O}_i(\epsilon)$ it is $\beta_i < \epsilon$, so the condition $\beta_i < \zeta(q)$ is guaranteed as long as

$$\epsilon \le \min\left\{\min_{\mathscr{O}_i(\epsilon_{i0})}\zeta(q), \epsilon_{i0}\right\} \triangleq \epsilon_{i1}'$$

(The detailed expression of ϵ'_{i1} is found in [53, Lemma 4.12].)

For $\mathrm{D}_{h_2}(q, \lambda)$ now, one expands it to

$$\mathrm{D}_{h_2}(q,\lambda) = \underbrace{\sigma_i v_i \mathrm{I} - \sigma_i v_i \widehat{(q-q_i)}\widehat{(q-q_i)}^{\mathsf{T}}}_{\mathrm{D}_{h_{21}}(q,\lambda)}$$
$$+ \underbrace{(1-\sigma_i)\mathrm{I} + \frac{\sigma_i v_i}{1+\beta_i}(q-q_i)\nabla\beta_i^{\mathsf{T}} + \sum_{j=0, j\neq i}^{M} \{(v_j-1)\sigma_j \mathrm{I} + (q-q_j)[\sigma_j \nabla v_j + (v_j-1)\nabla\sigma_j]^{\mathsf{T}}\}}_{\mathrm{D}_{h_{22}}(q,\lambda)}$$

Working similarly in parts, separate $\mathrm{D}_{h_{21}}(q, \lambda)$ to show that it is always positive semidefinite:

$$\hat{y}^{\mathsf{T}}\mathrm{D}_{h_{21}}(q,\lambda)\hat{y} = \sigma_i v_i\left[1 - \left(\hat{x}\cdot\widehat{(q-q_i)}\right)^2\right] \geq 0$$

The second term, $\mathrm{D}_{h_{22}}(q, \lambda)$ can be *made* positive definite:

$$\mathrm{D}_{h_{22}}(q,\lambda) = \underbrace{\frac{\sigma_i v_i}{1+\beta_i}(q-q_i)\nabla\beta_i^{\mathsf{T}} + \sum_{j=0, j\neq i}^{M} \frac{\lambda(v_j-1)J_r(q,t)\bar{\beta}_i}{[J_r(q,t)\bar{\beta}_j + \lambda\beta_j]^2}(q-q_j)\nabla\beta_i^{\mathsf{T}}}_{\mathrm{D}_{h_{221}}(q,\lambda)}$$
$$+ \underbrace{(1-\sigma_i)\mathrm{I} + \sum_{j=0, j\neq i}^{M}\left\{\sigma_j(v_j-1)\mathrm{I} + \sigma_j(q-q_j)\nabla v_j^{\mathsf{T}} + \frac{\lambda\beta_i}{[J_r(q,t)\bar{\beta}_j + \lambda\beta_j]^2}\right\}X_{ij}^*(q)^{\mathsf{T}}}_{\mathrm{D}_{h_{222}}(q,\lambda)\triangleq H_i(q,\lambda)}$$

For the positive definiteness of $\hat{y}^{\mathsf{T}}\mathrm{D}_{h_{221}}\hat{y}$ it suffices to show

$$\begin{cases} \dfrac{\lambda v_i \| q-q_i \|}{3} > (1+\beta_j)J_r(q,t)\bar{\beta}_i \sum\limits_{j=0, j\neq i}^{M} \dfrac{|v_j-1|\,\|q-q_j\|}{\beta_j^2} \\ \dfrac{v_i \| q-q_i \|}{3} > (1+\beta_i)\beta_i \sum\limits_{j=0, j\neq i}^{M} \dfrac{|v_j-1|\,\|q-q_j\|}{\beta_j^2} \end{cases} \quad (13)$$

Recall that $q \in \mathcal{O}_i(\epsilon_{i0})$, and let $E_i \geq \epsilon_{i0}$ be the positive geometric constants of Definition 4. For $q \in \mathcal{O}_i(E_i)$, we have $\beta_i < E_i$ and $\beta_j > E_j$. The upper branch of (13) is satisfied for $\lambda > \Lambda_{i1}$ where

$$\Lambda_{i1} \triangleq \max_{\mathcal{O}_i(E_i)} \left\{ \frac{3(1+\beta_i) J_r(q,t) \bar{\beta}_i}{v_i \| q - q_i \|} \sum_{j=0, j\neq i}^{M} \frac{|v_j - 1| \, \| q - q_j \|}{\beta_j^2} \right\}$$

while the lower branch of (13) is satisfied by setting $E_i < \epsilon_{i1}$, where ϵ_{i1} is the (positive) solution of the second-order algebraic equation $x^2 + x + A = 0$ in which $A \triangleq \min_{\mathcal{O}_i(E_i)} \frac{v_i \| q - q_i \|}{3 \sum_{j=0, j\neq i}^{M} \frac{|v_j - 1| \, \| q - q_j \|}{\beta_j^2}}$. Detailed expressions for Λ_{i1} and ϵ_{i1} are in [53, Lemma 4.12].

Finally, to make $\mathrm{D}_{h_{222}}(q, \lambda)$ positive semidefinite, one directly applies [53, Lemma 4.11] —the adapted version of [1, Lemma B.1.2]. That lemma guarantees the existence of a continuous function $\Lambda_i^* : \mathcal{O}_i(E_i) \to \mathbb{R}_+$, for which if $\lambda \geq \max_{\mathcal{O}_i(E_i)} \Lambda_i^*(q) \triangleq \Lambda'_{i1}$, the bilinear form $\hat{u}^{\mathsf{T}} \mathrm{D}_{h_{222}}(q, \lambda) \hat{v}^{\mathsf{T}}$ is positive semidefinite for $0 < \hat{u} \cdot \hat{v} \leq 1$. To complete the proof, one then selects $\epsilon \leq \min_{i \in \{0, \ldots, M\}} \{\epsilon_{i1}, \epsilon'_{i1}\} < E_i$ and $\lambda \geq \max_{i \in \{0, \ldots, M\}} \{\Lambda_{i1}, \Lambda'_{i1}\}$. □

C. Proof of Lemma 6

Let $\hat{y} = y_1 + y_2$, where $y_1 \in \mathrm{span}\{q - q_i\}$ and $y_2 \in \mathrm{span}\{q - q_i\}^{\perp}$. Observe now that

$$\hat{y}_2^{\mathsf{T}} \mathrm{D}_{h_\lambda} \hat{y} \geq \underbrace{\frac{1}{2} v_i \| y_2 \| + \lambda J_r(q,t) \bar{\beta}_i (\nabla \beta_i \cdot \hat{y}) \times \sum_{j=0, j\neq i}^{M} \frac{(v_j - 1)[\hat{y}_2 \cdot (q - q_j)]}{(J_r(q,t)\bar{\beta}_j + \lambda \beta_j)^2}}_{K_1(q,\lambda,t)}$$
$$+ \underbrace{\sum_{j=0, j\neq i}^{M} \hat{y}_2^{\mathsf{T}} \left[(\sigma_j v_j - \sigma_j) \mathrm{I} + (q - q_j) \sigma_j \nabla v_j^{\mathsf{T}} + \frac{\lambda \beta_j X_{ij}^*(q)}{(J_r(q,t)\bar{\beta}_j + \lambda \beta_j)^2} \right] \hat{y} + \frac{1}{2} v_i \| y_2 \|}_{K_2(q,\lambda,t)}$$

Now $K_1(q, \lambda, t)$ is positive semidefinite if $\frac{\| y_2 \|}{\lambda} \left[\frac{1}{2} \lambda v_i - J_r(q,t) \bar{\beta}_i (\sqrt{2} + 1) \| \nabla \beta_i \| \sum_{j=0, j\neq i}^{M} \frac{|v_j - 1| \, \| q - q_j \|}{\beta_j^2} \right] > 0$, ensured for a sufficiently large λ:[3] $\lambda > \max_{\mathcal{O}_i(\epsilon_{i0})} \{\zeta'''(q)\} \triangleq \Lambda'_{i2}$. Now bound $K_2(q, \lambda, t)$ from below as

$$K_2(q,\lambda,t) \geq \frac{1}{2\sqrt{3}} v_i \widehat{\nabla \beta_i} \cdot \widehat{(q - q_i)} - \frac{\beta_i}{\lambda} \sum_{j=0 j\neq i}^{M} \{ \frac{J_r(q,t) \bar{\beta}_{ij} (|v_j - 1| + \| q - q_j \| \, \| \nabla v_j \|)}{\beta_j}$$ which

$$+ \frac{\| X_{ij}^*(q) \|}{\beta_j^2} \}$$

can be made positive semidefinite, if

[3] A detailed expression for $\zeta'''(q)$ is found in [53, Lemma 4.13].

$$\epsilon < \epsilon_{i2} \triangleq \min\left\{ \min_{\mathcal{O}_i(\epsilon_{i0})} \left\{ \widehat{\nabla \beta_i \cdot (q - q_i)} \right\}, \epsilon_{i0} \right\}$$

$$\lambda \geq \max\left\{ \max_{\mathcal{O}_i(\epsilon_{i0})} \{\zeta'(q,t)\}, \Lambda'_{i2} \right\} \triangleq \Lambda''_{i2}$$

making $K_2(q, \lambda, t)$ positive semidefinite. □

D. Proof of Lemma 7

For $q \in \mathscr{A}_{\mathscr{L}}(\epsilon)$, σ_j with $j \in \mathscr{L}$ is upper bounded by $\frac{1}{2 \mid \mathscr{L} \mid}$, and thus $\sigma_d = 1 - \Sigma_{j \in \mathscr{L}} \sigma_j \geq \frac{1}{2}$. Letting now $\delta'_0 \triangleq \left[2\max_{\mathscr{F}} \{ \Sigma_{j \in \mathscr{L}} (\| \mathrm{D}_{f_i} \| + \| f_j - q \|) \} \right]^{-1}$ and setting $\delta_0 \triangleq \min\{\delta'_0, \frac{1}{2 \mid \mathscr{L} \mid}\}$, one can pick $\Lambda_0(\epsilon) \triangleq \max_{j \in \{0, \ldots, M\}} \{N_{0j}(\epsilon, \delta_0), N_{1j}(\epsilon, \delta_0)\}$ and take $\mu \geq \Lambda_0$, so that $\mathrm{D}_{f_\mu} \hat{y} = \Sigma_{j \in \mathscr{L}} \left[\sigma_j \mathrm{D}_{f_j} + (f_j - q) \nabla \sigma_j^{\mathsf{T}} \right] \hat{y} + \sigma_d \hat{y}$ is bounded away from zero, making D_{f_μ} non-singular on $\mathscr{A}_{\mathscr{L}}(\epsilon) - \mathcal{S}$. □

E. Proof of Lemma 8

Pick an obstacle $\mathcal{O}_i$ and define a cone inside $T_q \mathscr{F}_w$, the tangent space of $\mathscr{F}$ at point q, as follows: $C_i \triangleq \{ y \in T_q \mathscr{F} : \| y_2 \| \leq r_i \| y_1 \| \}$ with r_i being a positive constant. Invoke the following supplemental lemma:

Lemma 9. *Given a star forest in $\mathscr{F}$, there are two positive constants Λ_i and ϵ_i, such that if $\mu \geq \Lambda_i$, then $\forall q \in \mathcal{O}_i(\epsilon_i) - \mathcal{S}$ and for any unit vector $\hat{y} \in C_i$, it is $\hat{y}^{\mathsf{T}} \mathrm{D}_{f_\mu}(q) y_1 > 0$.*

Proof. The Jacobian of the purging transformation is

$$\mathrm{D}_{f_\mu} = \sigma_i \mathrm{D}_{f_i} + \underbrace{(f_i - q) \nabla \sigma_i^{\mathsf{T}} + \frac{1}{2}(1 - \sigma_i)\mathrm{I}}_{\mathrm{D}_{F_1}} + \underbrace{\frac{1}{2}(1 - \sigma_i)\mathrm{I} + \sum_{j \in \mathscr{L} - \{i\}} \left\{ \sigma_j (\mathrm{D}_{f_j} - \mathrm{I}) + (f_j - q) \nabla \sigma_j^{\mathsf{T}} \right\}}_{\mathrm{D}_{F_2}}$$

For any ray scaling map $f_i(q) = v_i(q - q_i) + q_i$ and unit vector $\hat{y} = y_1 + y_2 \in C_i$, and with $\alpha_i \geq 0$ in $\mathcal{O}_{\epsilon_{i0}}$ for some appropriately small $\epsilon_{i0} > \epsilon_{i1} > 0$ [53, Lemma 5.6], $\mathrm{D}_{f_i} \cdot y_1 = \alpha_i (\widehat{q - q_i})(\widehat{q - q_i})^{\mathsf{T}} y_1$. It follows that $\hat{y}^{\mathsf{T}} \mathrm{D}_{f_i} y_1 = \left[y_1 \cdot (\widehat{q - q_i}) \right]^2 \alpha_i \geq 0$ for $q \in \mathcal{O}(\epsilon_{i1})$. Expand D_{F_1} into $(v_i - 1)(q - q_i) \nabla \sigma_i^{\mathsf{T}} + \frac{1}{2}(1 - \sigma_i)\mathrm{I}$ and note that for all $q \in \mathcal{O}_i(\epsilon_{i1})$ it is $v_i \leq 1$ [2,

Lemma D.2.1]. A sufficient condition for $\hat{y}^{\mathsf{T}}\mathrm{D}_{F_1}y_1 \geq 0$ is that

$\beta_i < \frac{\Delta_i}{\max_{\mathscr{F}}\{\parallel q-q_i\parallel\}\max_{\mathscr{O}_i(\epsilon_{i1})}\{\parallel \nabla(\bar{\beta}_i\tilde{\beta}_i)\parallel \Big/ (\bar{\beta}_i\tilde{\beta}_i)\}} \triangleq \epsilon_{i2}$. For D_{F_2}, and for a unit vector $\hat{y} = y_1 + y_2 \in C_i$, it is $\parallel y_1 \parallel^2 \geq \frac{1}{1+r_i^2} =: \Delta^2$. There exists $\Lambda_{i2}(\Delta) > 0$ [53, Lemma 5.8] such that if $\mu \geq \Lambda_{i2}(\Delta)$ it is $\hat{y}^{\mathsf{T}}\mathrm{D}_{F_2}y_1 \geq 0$ for all $q \in \mathscr{O}_i(E_i) - \mathscr{S}$. Set $\Lambda_i \triangleq \Lambda_{i2}(\Delta)$ and $\epsilon_i \triangleq \min\{\epsilon_{i1}, \epsilon_{i2}\}$. □

Given $\epsilon < \epsilon_{i1}$ and $\mu > \Lambda_{i1}$, Lemma 9 thus implies that $\mathrm{D}_{f_\mu}(q)\hat{y} \neq 0$, $\forall q \in \mathscr{O}_i(\epsilon_{i1}) - \mathscr{S}$ and $\hat{y} \in C_i$. The same be stated for vectors outside the cone C_i.

Lemma 10. *Consider a star forest $\mathscr{F}$, pick an obstacle $\mathscr{O}_i$ and take any unit vector $\hat{y} \in T_q\mathscr{F} - C_i$. Decompose $\hat{y}$ in two ways: $\hat{y} = y_1 + y_2 = z_1 + z_2$ with $y_1 \in \mathrm{span}\{q_i - q\}$, $y_2 \perp y_1$, $z_1 \in \mathrm{span}\,\nabla\beta_i$, $z_2 \perp z_1$. Then there exist a positive constant Λ_i such that for all $\mu \geq \Lambda_i$ and an appropriate $r_i > 0$, it is $\hat{y}^{\mathsf{T}}\mathrm{D}_{f_\mu}(q)z_2 > 0$.*

Proof. The Jacobian of f_μ is [2, Lemma D.1.4]

$$\mathrm{D}_{f_\mu} = \sigma_i\mathrm{D}_{f_i} + \underbrace{(f_i - q)\nabla\sigma_i^{\mathsf{T}} + \frac{1}{2}(1-\sigma_i)I}_{\triangleq [Df]_1} + \underbrace{\frac{1}{2}(1-\sigma_i)I + \sum_{j \in \mathscr{L}-\{i\}}\left\{\sigma_j(\mathrm{D}_{f_j} - I) + (f_j - q)\nabla\sigma_j^{\mathsf{T}}\right\}}_{\triangleq [Df]_2}$$

Since $|\,\hat{x}\cdot(q-q_i)\,| = \parallel x_1\parallel\,\parallel q-q_i\parallel$, it holds that $\hat{x}^{\mathsf{T}}\left[D_{f_i}\right]y_2 \geq \parallel y_2\parallel(v_i\parallel y_2\parallel - \parallel x_1\parallel\,\parallel q-q_i\parallel\,\parallel\nabla v_i\parallel)$ and thus $\hat{x}^{\mathsf{T}}\left[Df_i\right]y_2 \geq 0$ if $\parallel y_2\parallel > v_i^{-1}\parallel q-q_i\parallel\,\parallel\nabla v_i\parallel\,\parallel x_1\parallel$. For $\hat{x} \in T_q\mathscr{F} - C_q$, there is some $r_i \equiv r_{i1}$, for which $\|x_2\| > r_{i1}\|x_1\|$.[4] Let this

$$r_{i1} \triangleq \left[\frac{1}{2}\left(1 - \sqrt{1 - [\widehat{\nabla\beta_i}\cdot(\widehat{q-q_i})]^2}\right)\right]^{-1}$$

From the definition of the star-shape collar, $\widehat{\nabla\beta_i}\cdot(\widehat{q-q_i}) \geq \frac{\Delta_i}{\max_{\mathscr{F}}\{\parallel\nabla\beta_i\parallel\}\max_{\mathscr{F}}\{\parallel q-q_i\parallel\}} \triangleq \hat{\Delta}_i > 0$, from which (cf. [53, (5.18)]) it then follows that $\parallel y_2\parallel^2 \geq \{1 - \frac{1}{4}(\sqrt{1-\hat{\Delta}_i^2}+1)^2\}\parallel x_2\parallel^2$ and consequently,

[4] Invoke [53, Lemma 5.10] with $u = (\widehat{q-q_i})$ and $v = \widehat{\nabla\beta_i}$.

$\| x_2 \| \sqrt{1-\frac{1}{4}(\sqrt{1-\hat{\Delta}_i^2}+1)^2} > \frac{\| q-q_i \| \ \| \nabla \beta_i \|}{v_i} \| x_1 \|$. One can then enlarge the cone C_q with $\|x_2\| > r_{i2}\|x_1\|$ using

$$r_{i2} \triangleq \frac{\max_{\mathscr{F}}\{ \| q-q_i \| \} \max_{\mathscr{O}_i(E_i)}\{ \| \nabla v_i \| \ / v_i \}}{\sqrt{1-\frac{1}{4}(\sqrt{1-\hat{\Delta}_i^2}+1)^2}}$$

The term $\max_{\mathscr{O}_i(E_i)}\{ \| \nabla v_i \| \ / v_i \}$ can be upper bounded [53, Lemma 5.11]. Now expanding $[Df]_1 = \frac{\mu}{\bar{\beta}_i\tilde{\beta}_i + \mu\beta_i}\left\{\frac{1}{2}\beta_i I + \frac{v_i - 1}{\bar{\beta}_i\tilde{\beta}_i + \mu\beta_i}(\beta_i(q-q_i)\nabla(\bar{\beta}_i\tilde{\beta}_i)^\intercal - \bar{\beta}_i\tilde{\beta}_i(q-q_i)\nabla\beta_i^\intercal)\right\}$ and with $y_2 \perp \nabla\beta_i$, one has the bound for the bilinear form $\hat{x}^\intercal[Df]_1 y_2 \geq \frac{\mu\beta_i \| y_2 \|}{\bar{\beta}_i\tilde{\beta}_i + \mu\beta_i}\left\{\frac{1}{2}\| y_2 \| - \frac{| v_i - 1 |}{\bar{\beta}_i\tilde{\beta}_i + \mu\beta_i} \| x_1 \| \ \| q-q_i \| \ \| \nabla(\bar{\beta}_i\tilde{\beta}_i) \|\right\}$, the positive semidefiniteness of which is implied by $\bar{\beta}_i\tilde{\beta}_i \| y_2 \| \geq 2 | v_i - 1 | \ \| q-q_i \| \ \| \nabla(\bar{\beta}_i\tilde{\beta}_i) \| \ \| x_1 \|$. Maximizing $\|y_2\|$ using the bound involving $\hat{\Delta}_i$, one can further inflate the cone C_q with $\|x_2\| \geq r_{i3}\|x_1\|$ using

$$r_{i3} \triangleq \frac{2\max_{\mathscr{O}_i(E_i)} | v_i - 1 | \ \| q-q_i \| \cdot \max_{\mathscr{O}_i(E_i)} \frac{\| \nabla(\bar{\beta}_i\tilde{\beta}_i) \|}{(\bar{\beta}_i\tilde{\beta}_i)}}{\sqrt{1-\frac{1}{4}(\sqrt{1-\hat{\Delta}_i^2}+1)^2}}$$

For $[Df]_2$, verify first that $\| y_2 \|^2 \geq 1-\frac{1}{4}(\sqrt{1-\hat{\Delta}_i^2}+1)^2$ and set (cf. [53, Lemma 5.8]) $\Delta \triangleq \sqrt{1-\frac{1}{4}(\sqrt{1-\hat{\Delta}_i^2}+1)^2}$ to force $\hat{x}^\intercal[Df]_2 y_2 \geq 0$. The proof is completed by choosing

$$r_i \triangleq \max\{r_{i1}, r_{i2}, r_{i3}\} \quad \Lambda_i \triangleq \Lambda_i(\Delta)$$

□

The same process that was used in the proof of Lemma 10 applies here to lead to the conclusion that $\mathrm{D}_{f_\mu}(q)\hat{y} \neq 0$ for $\hat{y} \notin C_i$. The two lemmas together suggest a choice of

$$\epsilon_i \triangleq \min\{\epsilon_{i1}, E_i\} \quad \Lambda_i \triangleq \max\{\Lambda_{i1}, \Lambda_{i2}\}$$

to make $\mathrm{D}_{f_\mu}(q)$ nonsingular in $\mathscr{O}(\epsilon) - \mathscr{S}$ as long as $\epsilon < \epsilon_i$ and $\mu \leq \Lambda_i$. □

Biographies

Caili Li graduated from Beijing Institute of Technology in Aerospace Engineering before earning his Master of Science in Mechanical Engineering at the University of Delaware. He is currently with AutoX Technologies Inc., a self-driving car technology company in the Silicon Valley, and focuses on path planning and human-AI hybrid control system development.

Herbert (Bert) Tanner received his Ph.D. in mechanical engineering from the National Technical University of Athens, Greece, in 2001. He was a postdoctoral researcher with the GRASP Lab at the University of Pennsylvania from 2001 to 2003, and subsequently became an assistant professor with the Department of Mechanical Engineering at the University of New Mexico. He is currently a professor of mechanical engineering at the University of Delaware.

Tanner received NSF's Career award in 2005. He is a fellow of the ASME, and a senior member of IEEE. He has served in the editorial boards of the IEEE Transactions on Automatic Control, the IEEE Robotics and Automation Magazine and the IEEE Transactions on Automation Science and Engineering. He is currently an associate editor for Automatica, and for Nonlinear Analysis Hybrid Systems, and a chief specialty editor for Frontiers in Robotics and AI: multi-robot systems.

References

[1]. Rimon E, "Exact robot navigation using artificial potential functions," Ph.D. dissertation, Yale Univ., New Heaven, CT, 1990.

[2]. Rimon E and Koditschek DE, "Exact robot navigation using artificial potential functions," IEEE Transactions on Robotics and Automation, vol. 8, no. 5, pp. 501–518, 1992.

[3]. Osorio-Comparan R et al., "Mobile robot navigation using potential fields and LMA," in Proceedings of the IEEE International Conference Automatica, 2016, pp. 1–7.

[4]. Borenstein J and Koren Y, "Real-time obstacle avoidance for fast mobile robots," IEEE Trans. Syst., Man, Cybern, vol. 19, no. 5, pp. 1179–1187, 1989.

[5]. Song P and Kumar V, "A potential field based approach to multi-robot manipulation," in Proceedings of the IEEE International Conference on Robotics and Automation, vol. 2, 2002, pp. 1217–1222.

[6]. Badawy A, "Manipulator trajectory planning using artificial potential field," in Proceedings of the International Conference on Engineering and Technology, 2014, pp. 1–6.

[7]. Ataka A, Qi P, Liu H, and Althoefer K, “Real-time planner for multi-segment continuum manipulator in dynamic environments,” in Proceedings of the IEEE International Conference on Robotics and Automation, 2016, pp. 4080–4085.

[8]. Khatib O, “Real-time obstacle avoidance for manipulators and mobile robots,” in Proceedings of the IEEE International Conference on Robotics and Automation, vol. 2, 1985, pp. 500–505.

[9]. Koren Y and Borenstein J, “Potential field methods and their inherent limitations for mobile robot navigation,” Proceedings of the IEEE International Conference on Robotics and Automation, pp. 1398–1404, 1991.

[10]. Tsourveloudis NC, Valavanis K, and Hebert T, “Autonomous vehicle navigation utilizing electrostatic potential fields and fuzzy logic,” IEEE Transactions on Robotics and Automation, vol. 17, no. 4, pp. 490–497, 2001.

[11]. Tuazon JPC et al., “An improved collision avoidance scheme using artificial potential field with fuzzy logic,” in Proceedings of the IEEE Region 10 Conference, 2016, pp. 291–296.

[12]. Janabi-Sharifi F and Vinke D, “Robot path planning by integrating the artificial potential field approach with simulated annealing,” in Proceedings of the IEEE Systems Man and Cybernetics Conference, 1993, pp. 282–287.

[13]. Bentes C and Saotome O, “Dynamic swarm formation with potential fields and a* path planning in 3d environment,” in Proceedings of the Latin American Robotics Symposium, 2012, pp. 74–78.

[14]. Wallar A and Plaku E, “Path planning for swarms by combining probabilistic roadmaps and potential fields,” in Lecture Notes in Artificial Intelligence. Berlin, Germany: Springer, 2014, pp. 417–428.

[15]. Amiryan J and Jamzad M, “Adaptive motion planning with artificial potential fields using a prior path,” in Proceedings of the 3rd International Conference on Robotics and Mechatronics, 2015, pp. 731–736.

[16]. Cerqueira TA, Santos TLM, and Conceicao AGS, “A new approach based in potential fields with obstacles avoidance for mobile robots,” in Proceedings of the Latin American Robotics Symposium, 2016, pp. 229–233.

[17]. Li P and Horowitz R, “Passive velocity field control of mechanical manipulators,” IEEE Transactions on Robotics and Automation, vol. 15, no. 4, pp. 751–763, 1999.

[18]. Cervantes I et al., “A robust velocity field control,” IEEE Trans. Control Syst. Technol, vol. 10, no. 6, pp. 888–894, 2002.

[19]. Moreno J and Kelly R, “Hierarchical velocity field control for robot manipulators,” in Proceedings of the IEEE International Conference on Robotics and Automation, vol. 3, 2003, pp. 4374–4379.

[20]. Dixon W et al., “Adaptive velocity field control of a wheeled mobile robot,” in Proceedings of the 5th International Workshop on Robot Motion and Control, 2005, pp. 145–150.

[21]. Yamakita M et al., “An application of passive velocity field control to cooperative multiple 3-wheeled mobile robots,” in Proceedings of the IEEE/RSJ International Conference on Intelligent Robots and Systems, vol. 1, 1998, pp. 368–373.

[22]. LaValle SRL and M. S, “Simple and efficient algorithms for computing smooth, collision-free feedback laws over given cell decompositions,” Int. J. Robot. Res, vol. 28, no. 5, pp. 600–621, 2009.

[23]. Lerner J, Wagner D, and Zweig KA, Eds., Algorithmics of Large and Complex Networks, ser. Lecture Notes in Computer Science. Berlin, Germany: Springer, 2009, vol. 5515.

[24]. Karaman S and Frazzoli E, “Sampling-based algorithms for optimal motion planning,” The International Journal of Robotics Research, vol. 30, no. 7, pp. 846–894, 2011.

[25]. Belkhouche F, Belkhouche B, and Rastgoufard P, “Line of sight robot navigation toward a moving goal,” IEEE Transactions on Systems, Man, and Cybernetics B, vol. 36, no. 2, pp. 255–267, 2006.

[26]. Matveev A, Hoy M, and Savkin A, “Real-time kinematic navigation of a mobile robot among moving obstacles with guaranteed global convergence,” in Proceedings of the IEEE International Conference on Robotics and Biomimetics, 2014, pp. 2146–2151.

[27]. Connolly CI, Burns JB, and Weiss R, “Path planning using laplace’s equation,” in Proceedings of the IEEE International Conference on Robotics and Automation, 1990, pp. 2102–2106.

[28]. Kim JO and Khosla P, “Real-time obstacle avoidance using harmonic potential functions,” in Proceedings of the IEEE International Conference on Robotics and Automation, 1991, pp. 790–796.

[29]. Kim JO and Khosla PK, “Real-time obstacle avoidance using harmonic potential functions,” IEEE Transactions on Robotics and Automation, vol. 8, no. 3, pp. 338–349, 1992.

[30]. Feder HJS and Slotine JJE, “Real-time path planning using harmonic potentials in dynamic environments,” in Proceedings of the IEEE International Conference on Robotics and Automation, vol. 1, 1997, pp. 874–881.

[31]. Szulczynski P, Pazderski D, and Kozlowski K, “Real-time obstacle avoidance using harmonic potential functions,” Journal of Automation Mobile Robots and Intellent Systems, vol. 5, no. 3, pp. 59–66, 2011.

[32]. Petres C, Paihas Y, Patron P, Petillot Y, Evans J, and Lane D, “Path planning for autonomous underwater vehicles,” IEEE Transactions on Robotics, vol. 23, no. 2, pp. 331–341, 2007.

[33]. Shah SK and Tanner HG, “Dynamics-compatible potential fields using stochastic perturbations,” in Proceedings of the 23rd IEEE Mediterranean Conference on Control and Automation, 2015, pp. 278–283.

[34]. Tanner HG, Loizou SG, and Kyriakopoulos KJ, “Nonholonomic navigation and control of cooperating mobile manipulators,” IEEE Transactions on Robotics and Automation, vol. 19, no. 1, pp. 53–64, 2003.

[35]. Loizou SG and Kyriakopoulos KJ, “Motion planning of piezoelectrically driven micro-robots via navigation functions,” in Proceedings of the IEEE Mediterrean Conference on Control and Automation, 2005, pp. 826–831.

[36]. Loizou SG and Kyriakopoulos KJ, “A feedback-based multiagent navigation framework,” International Journal of System Science, vol. 37, no. 6, pp. 377–384, 2006.

[37]. Conner D, Rizzi A, and Choset H, “Composition of local potential functions for global robot control and navigation,” in Proceedings of the 2003 IEEE/RSJ International Conference on Intelligent Robots and Systems, 2003, pp. 3546–3551.

[38]. Cui SS and Ge Y, “Dynamic motion planning for mobile robots using potential field method,” Autonomous Robots, vol. 13, pp. 207–222, 2002.

[39]. Kamel MA and Zhang Y, “Decentralized leader-follower formation control with obstacle avoidance of multiple unicycle mobile robots,” in Proceedings of the 28th IEEE Canadian Conference on Electrical and Computer Engineering, 2015, pp. 406–411.

[40]. Nakazawa K, Takahashi K, and Kaneko M, “Unified environment-adaptive control of accompanying robots using artificial potential field,” in Proceedings of the ACM/IEEE International Conference on Human-Robot Interaction, 2013, pp. 199–200.

[41]. Kasim FM and Jisha VR, “Lyapunov based approach for target tracking control of a mobile robot,” in Proceedings of the IEEE International Conference on Electrical, Computer and Communication Technologies, 2015, pp. 1–6.

[42]. Hui NB, “Coordinated motion planning of multiple mobile robots using potential field method,” in Proceedings of the International Conference on Industrial Electronics, Control and Robotics, 2010, pp. 6–11.

[43]. Jaradat MAK, Garibeh MH, and Feilat EA, “Dynamic motion planning for autonomous mobile robot using fuzzy potential field,” in Proceedings of the 6th International Symposium on Mechatronics and its Applications, 2009, pp. 1–6.

[44]. Jaradat MAK, Garibeh MH, and Feilat EA, “Autonomous mobile robot dynamic motion planning using hybrid fuzzy potential field,” Soft Computing, vol. 16, no. 1, pp. 153–164, 2012.

[45]. Li G et al., “Improved artificial potential field-based simultaneous forward search method for robot path planning in complex environment,” in Proceedings of the IEEE/SICE International Symposium on System Integration, 2015, pp. 760–765.

[46]. Philippsen R and Siegwart R, “An interpolated dynamic navigation function,” in Proceedings of the 2005 International Conference on Robotics and Automation, 2005, pp. 3782–3789.

[47]. Sun J and Tanner HG, “Constrained decision-making for low-count radiation detection by mobile sensors,” Autonomous Robots, vol. 39, no. 4, pp. 519–536, 2015.

[48]. Panagou D and Kumar V, “Maintaining visibility for leader-follower formations in obstacle environments,” in Proceedings of the IEEE International Conference on Robotics and Automation, 2012, pp. 1811–1816.

[49]. Panagou D and Kumar V, “Cooperative visibility maintenance for leader-follower formations in obstacle environments,” IEEE Transactions on Robotics, vol. 30, no. 4, pp. 831–844, 2014.

[50]. Panagou D, “Motion planning and collision avoidance using navigation vector fields,” in Proceedings of the IEEE Internationa Conference on Robotics and Automation, 2014, pp. 2513–2518.

[51]. Valbuena L and Tanner HG, “Hybrid potential field based control of differential drive mobile robots,” Journal of Intelligent & Robotic Systems, vol. 68, no. 3–4, pp. 307–322, 2012.

[52]. Fernandez-Guasti M, “Analytic geometry of some rectilinear figures,” Int. J. Math. Ed. Sci. Tech, vol. 23, pp. 895–901, 1992.

[53]. Li C, “Star-world navigation functions for convergence to a time-varying destination manifold,” Master’s thesis, Univ. of Delaware, Newark, DE, 2017.

[54]. Koditschek DE and Rimon E, “Robot navigation functions on manifolds with boundary,” Advances in Applied Mathematics, vol. 11, no. 4, pp. 412–442, 1990.

[55]. Constantine G and Savits T, “A multivariate Faá di Bruno formula with applications,” Trans. Am. Math. Soc, vol. 348, no. 2, pp. 503–520, 1996.

[56]. Johnson WP, “The curious history of Faá di Bruno’s formula,” The American Mathematical Monthly, vol. 109, no. 3, pp. 217–234, 2002.

[57]. Li C. Potential function. [Online]. Available: https://github.com/licaili193/potential_function

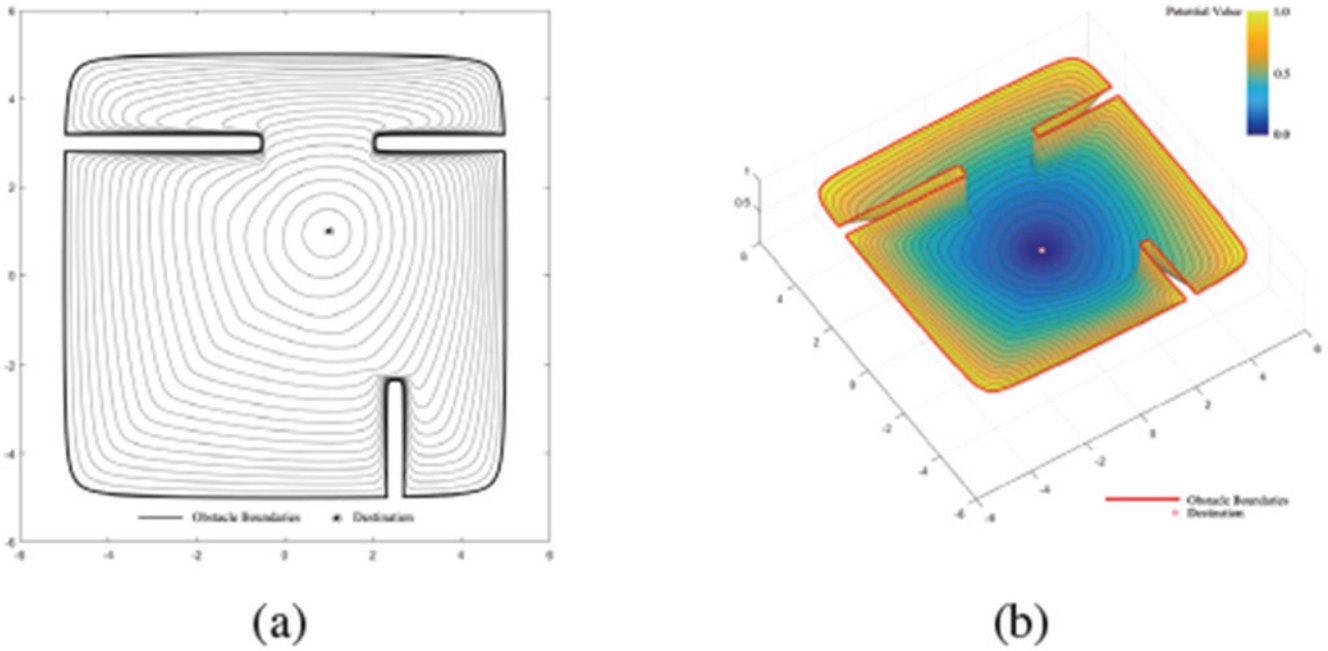

Fig. 1:
An example of a potential field generated by a navigation function in a simple rectangular environment: (a) contour plot, and (b) three dimensional rendering.

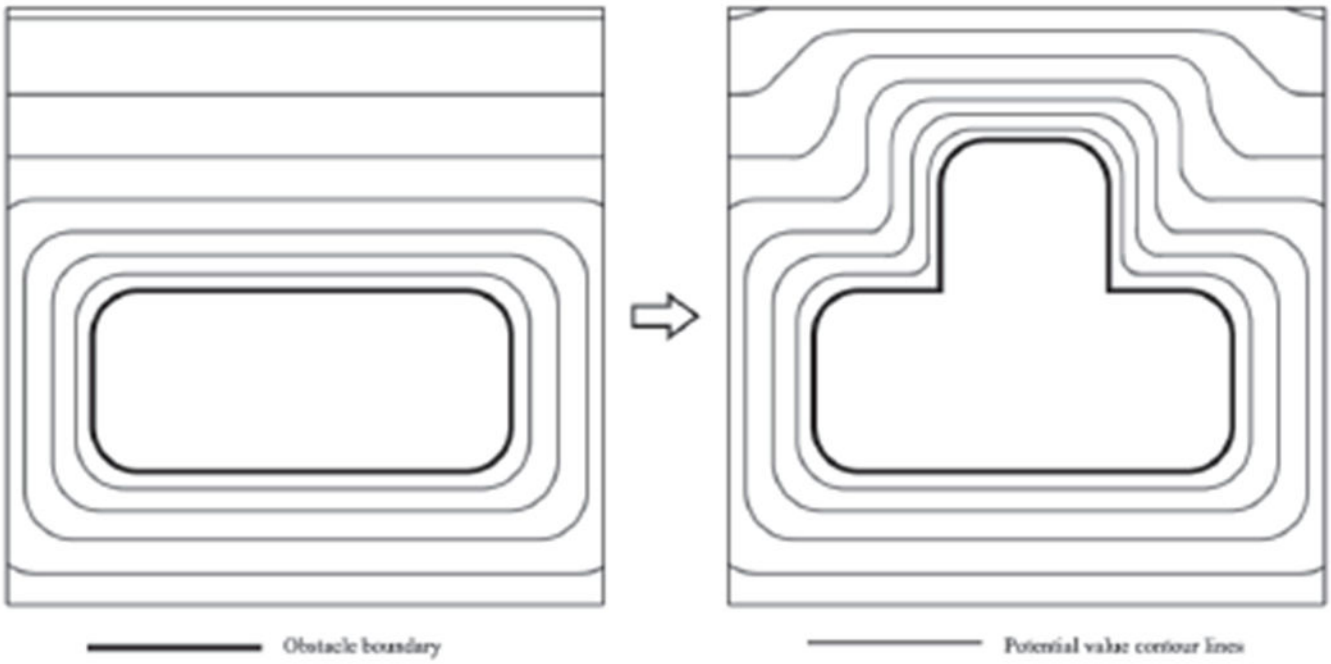

Fig. 2:

How the purging transformation works. Intersecting star shapes form a parent-child hierarchy, and then the inverse of the transformation shown above draws the interior of the child within its parent, and maps the boundary of the child to the portion of the boundary of the parent which is in the overlap of the two shapes.

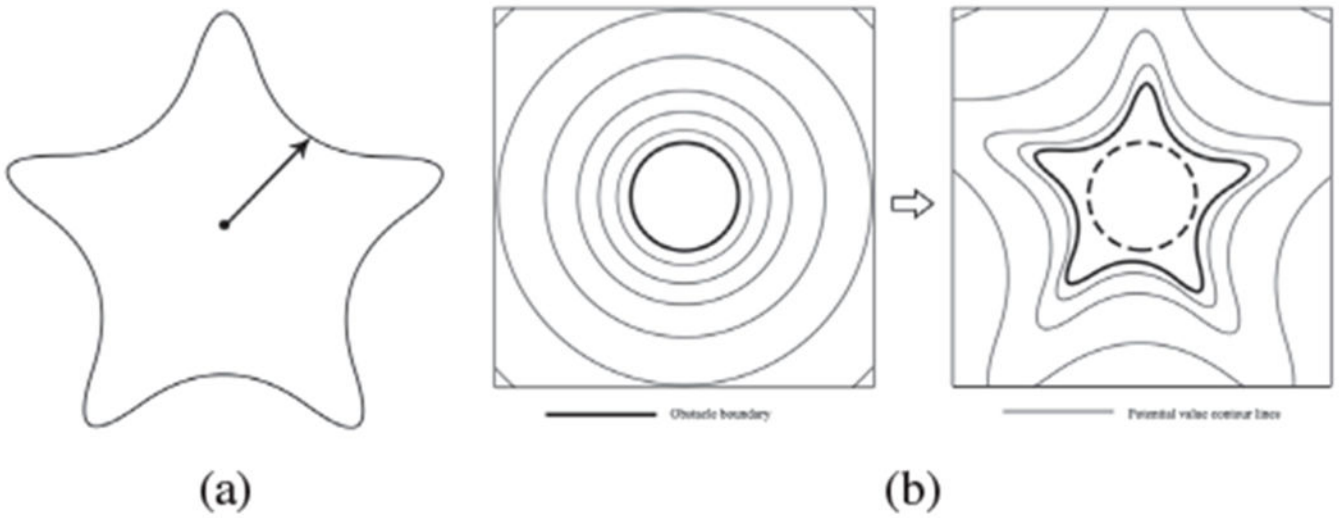

Fig. 3:

(a) an example of a star shape; all points on the boundary are “visible” from an interior point called the *center*, i.e., the ray from center to boundary does not intersect the boundary anywhere else. (b) the (inverse of a) star-to-sphere transformation is a bijective mapping that relates the boundary of a star to that of a sphere.

Fig. 4:
The pediatric rehabilitation clinical study environment.

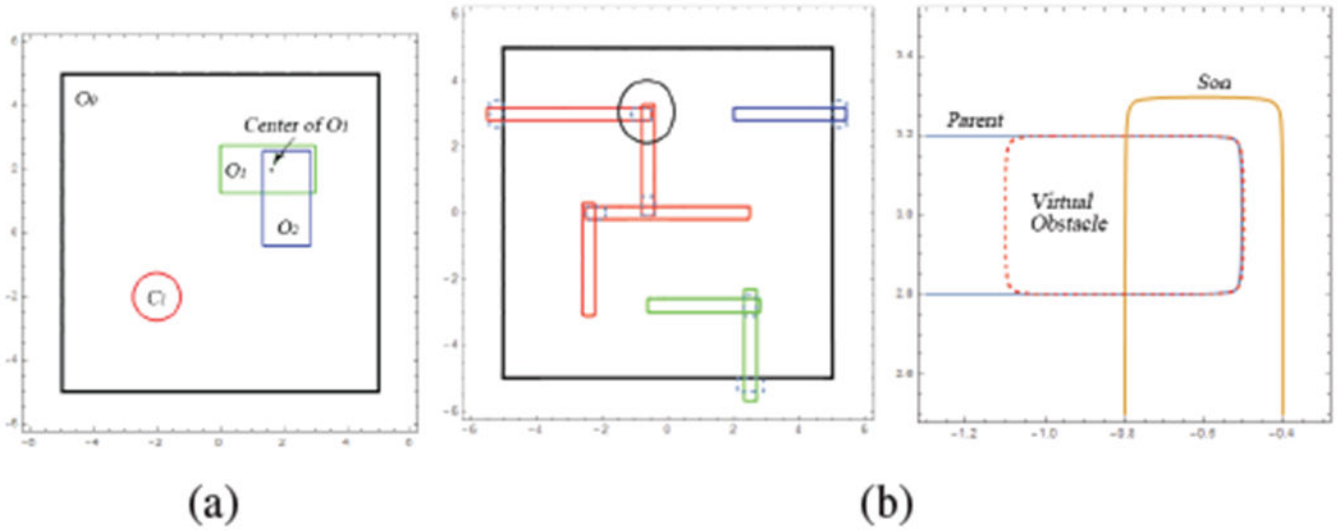

Fig. 5:

(a) Environment layout for the first simulation study. (b) Environment layout for the second simulation study (left), and a zoomed view of the circled area (right).

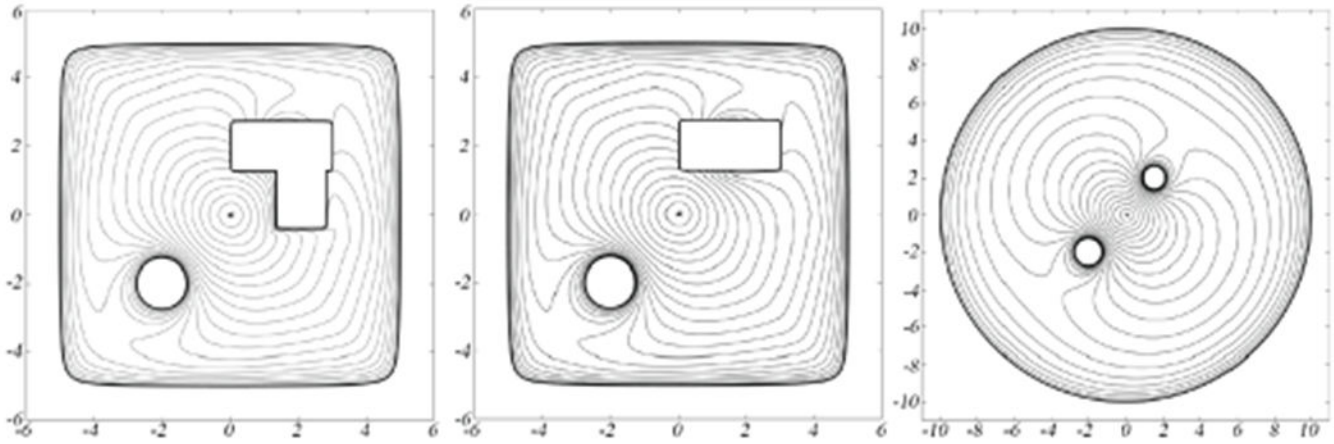

Fig. 6:

Time-varying navigation functions of the first example: the resulting navigation function (left), the modeling star world navigation function after applying a purging transformation (middle), and the modeling sphere world navigation function after applying a star-to-sphere transformation (right).

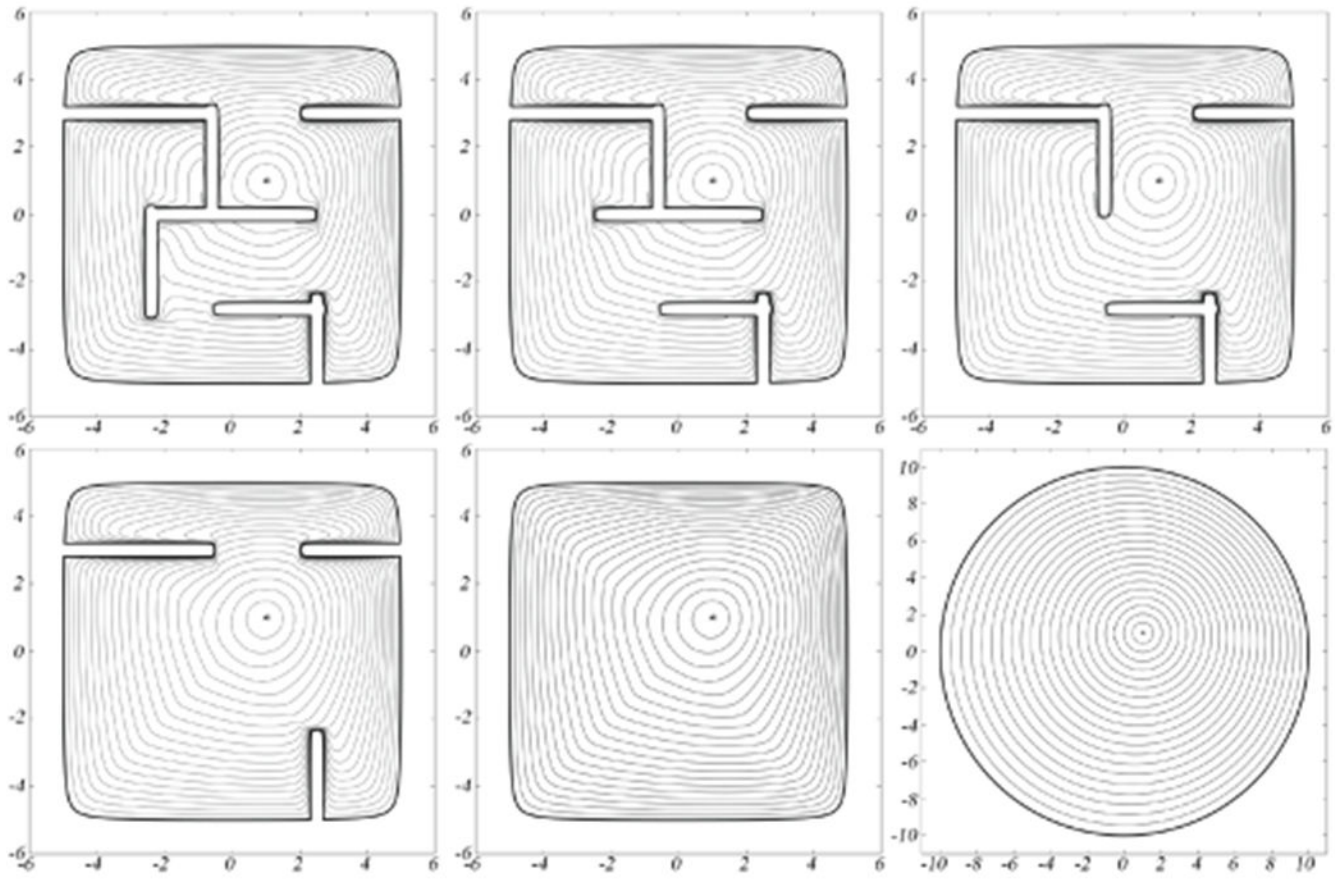

Fig. 7:

Time-varying navigation functions of the second example from the resulting navigation function in star forests to its the modeling sphere world navigation function.

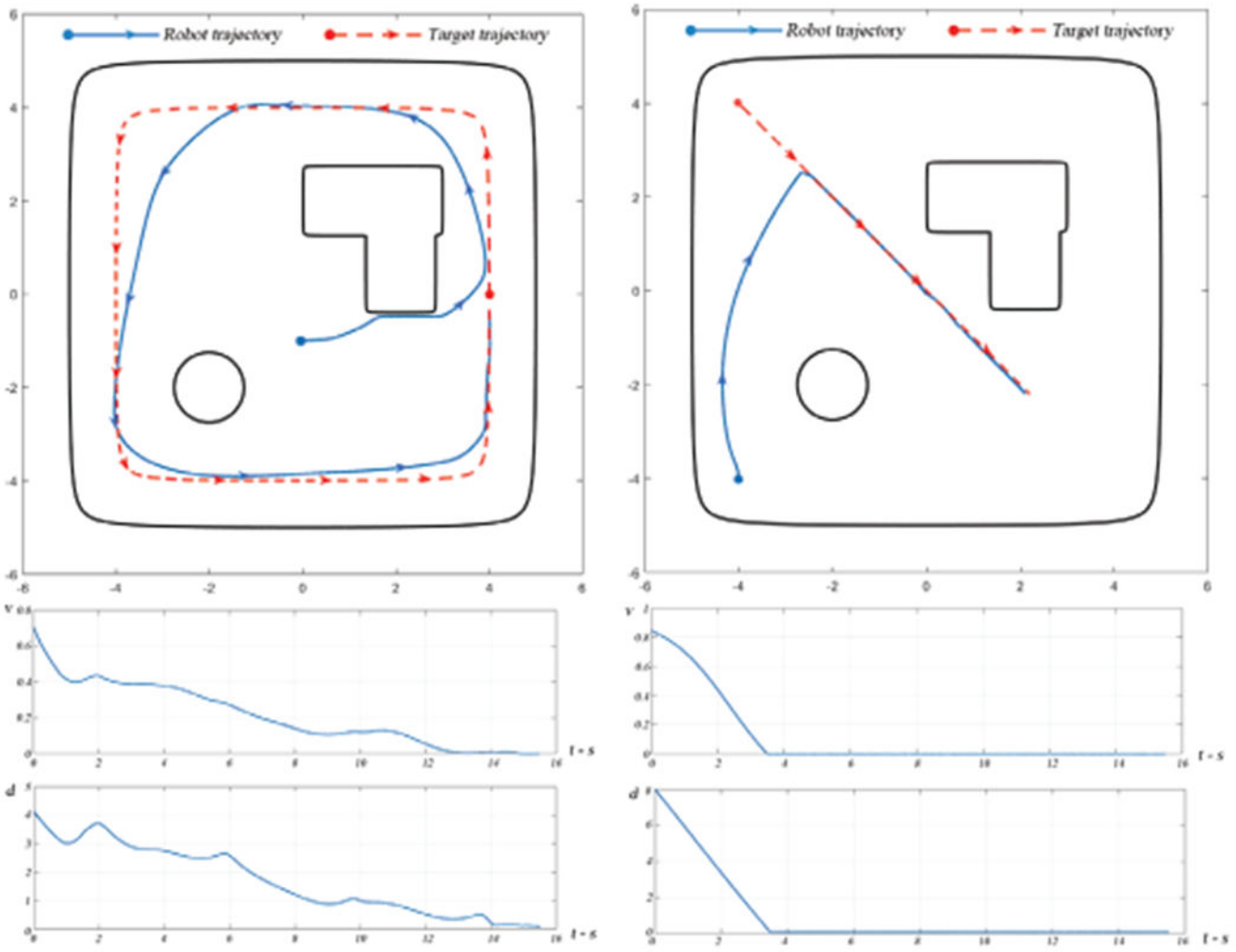

Fig. 8:

Simulations for different target movement and initial robot configurations. The paths of target and robot are shown in the figures on the upper row, and the evolution of the artificial potential v and robot-target d is shown, for each case, in the bottom row.

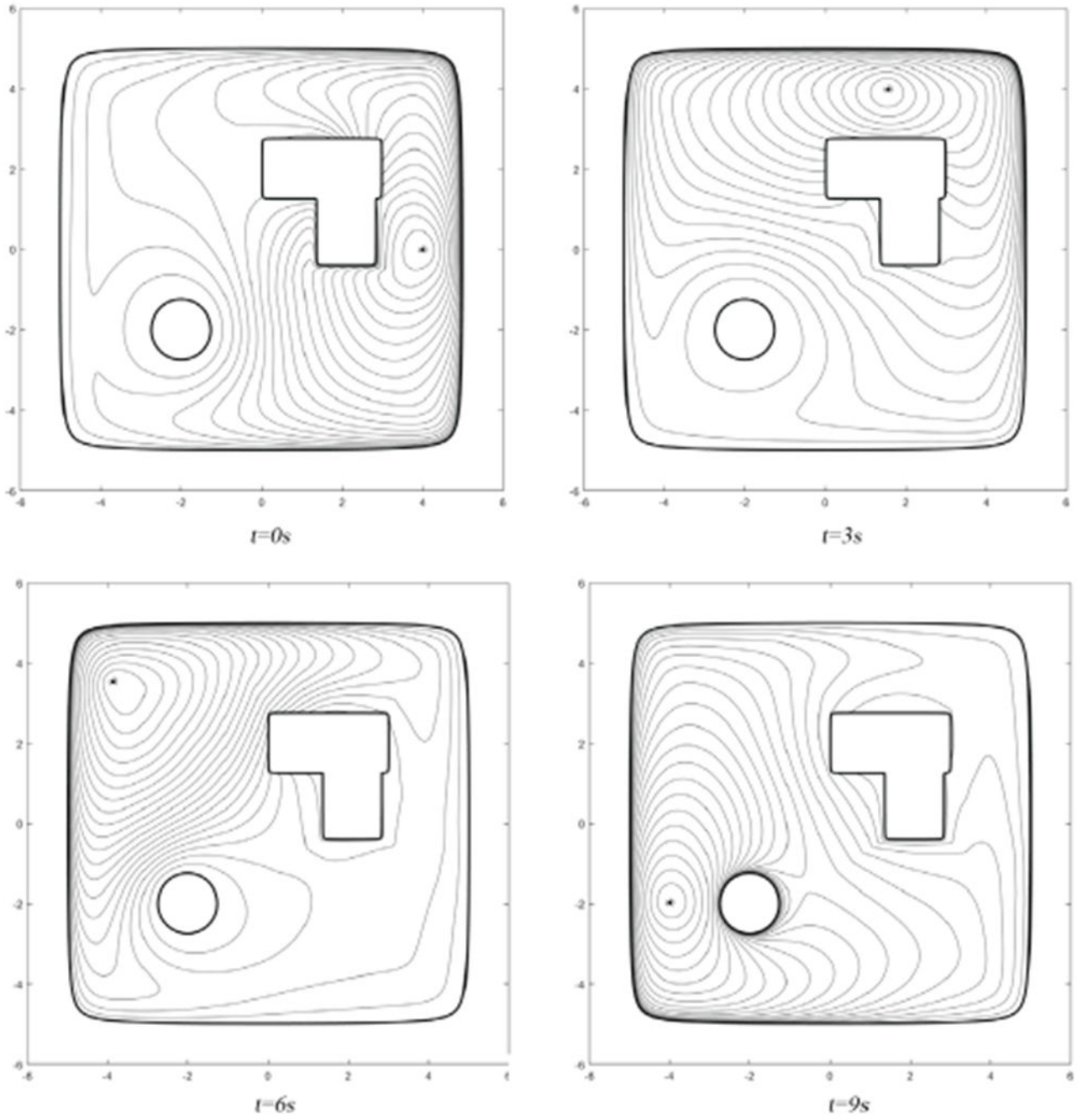

Fig. 9:
Contour plots of the time-varying navigation function at different instances of simulation time, as the target moves around in the workspace.

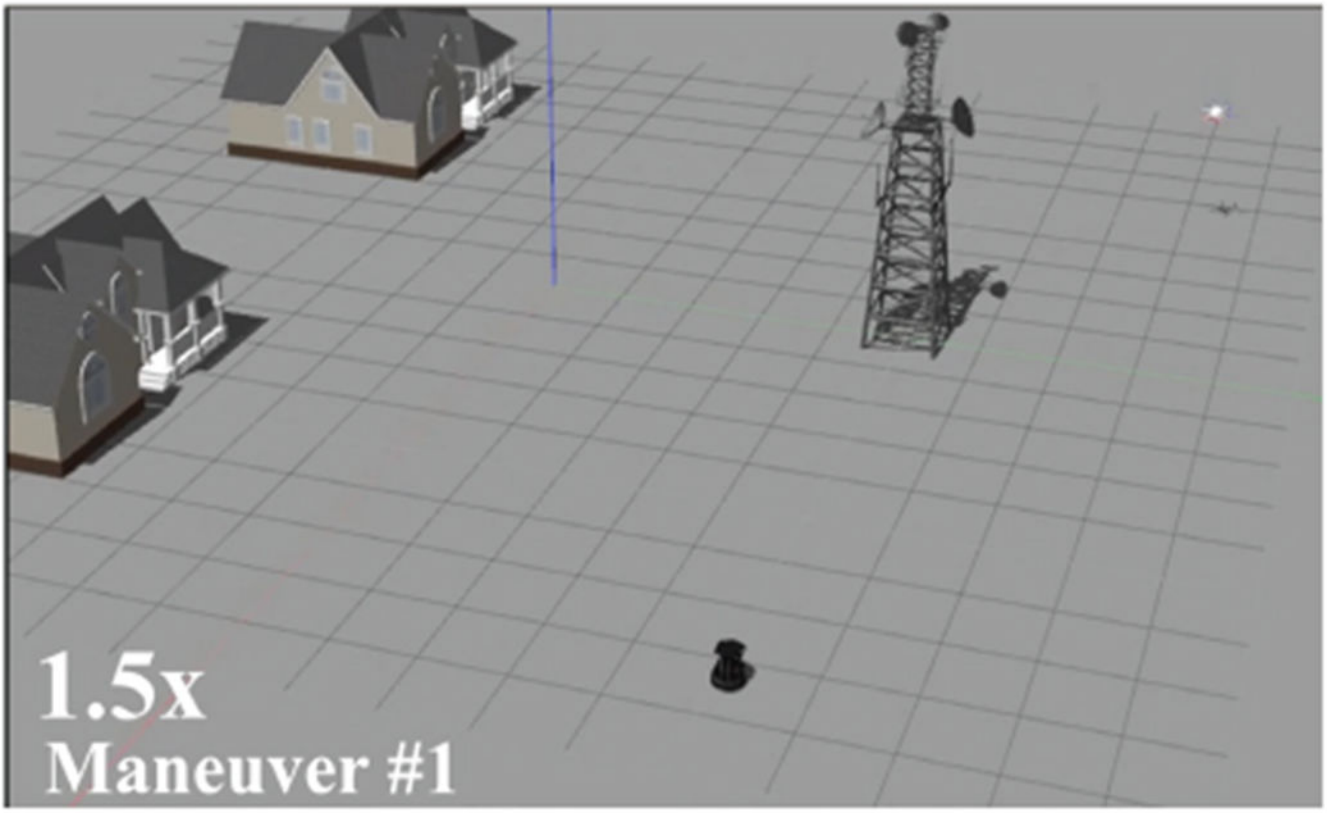

Fig. 10:
GAZEBO simulation of a quadrotor (top right) intercepting a moving ground target (bottom center). The time-varying navigation function provides motion directions to the aerial vehicle.

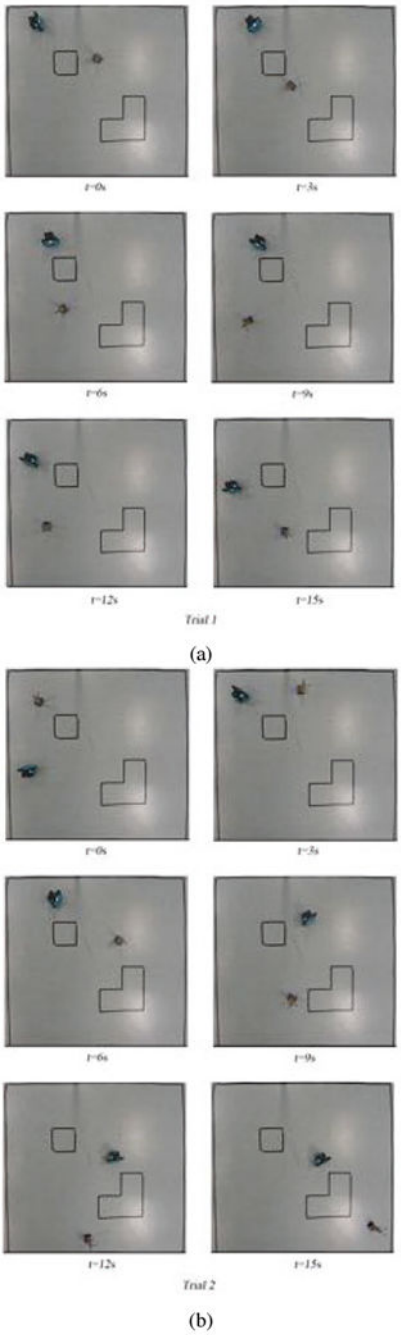

Fig. 11:
Two experimental trials with a unicycle robot (larger robot) chasing a moving target (smaller robot).